Dissertation

REAL-TIME IMAGING OF MITOCHONDRIAL ATP DYNAMICS ALLOWS METABOLIC PROFILING OF INDIVIDUAL CELLS

submitted by

BSc MSc

Maria Rosa DEPAOLI

for the Academic Degree of

Doctor of Philosophy

(PhD)

at the

Medical University of Graz

Gottfried Schatz Research Center

Molecular Biology and Biochemistry

under the Supervision of

Assoc. Prof. Mag. Dr. Roland Malli

2018

Statutory Declaration

I hereby declare that this thesis is my own original work and that I have acknowledged by name all who have made a contribution. Furthermore all sources used for the preparation of the thesis are cited. Throughout this thesis and for all related publications, I followed the Standards of Good Scientific Practice and Ombuds Committee at the Medical University of Graz.

Graz, October 30th, 2018 *Maria Depaoli e.h.*

Disclosures

Part of this thesis has been published in:

Depaoli MR, Karsten F, Madreiter-Sokolowski CT, Klec C, Gottschalk B, Bischof H, Eroglu E, Waldeck-Weiermair M, Simmen T, Graier WF, Malli R. Real-time imaging of mitochondrial ATP dynamics discloses the metabolic setting of single cells. Cell Reports 2018, https://doi.org/10.1016/j.celrep.2018.09.027.

The following co-authors contributed to my first-author publication:

Felix Karsten[1], Corina T. Madreiter-Sokolowski[1], Christiane Klec[1], Benjamin Gottschalk[1], Helmut Bischof[1], Emrah Eroglu[1], Markus Waldeck-Weiermair[1], Thomas Simmen[2], Wolfgang F. Graier[1], Roland Malli[1]

[1]Medical University of Graz, Neue Stiftingtalstraße 6/6, 8010 Graz, Austria
[2]University of Alberta, T6G 2H7 Edmonton, Canada

I confirm that all co-authors have agreed to use their data in my thesis. I have permission from the publisher to reproduce figures published in Depaoli et al. (2018).

During my PhD thesis I also contributed to the following publications:

- Depaoli MR, Hay J, Graier WF, Malli R. The enigmatic ATP supply of the endoplasmic reticulum. Biological Reviews 2018.
- Bernhart E, Kogelnik N, Prasch J, Gottschalk B, Goeritzer M, Depaoli MR, Reicher H, Nusshold C, Plastira I, Hammer A, Fauler G, Malli R, Graier WF, Malle E, Sattler W. 2-Chlorohexadecanoic acid induces ER stress and mitochondrial dysfunction in brain microvascular endothelial cells. Redox Biology 2018.

- Eroglu E, Charoensin S, Bischof H, Ramadani J, Gottschalk B, Depaoli MR, Waldeck-Weiermair M, Graier WF, Malli R. Genetic biosensors for imaging nitric oxide in single cells. Free Radical Biology and Medicine 2018.
- Charoensin S, Eroglu E, Opelt M, Bischof H, Madreiter-Sokolowski CT, Kirsch A, Depaoli MR, Frank S, Schrammel A, Mayer B, Waldeck-Weiermair M, Graier WF, Malli R. Intact mitochondrial Ca^{2+} uniport is essential for agonist-induced activation of endothelial nitric oxide synthase (eNOS). Free Radical Biology and Medicine 2017.
- Eroglu E, Rost R, Bischof H, Blass S, Schreilechner A, Gottschalk B, Depaoli MR, Klec C, Charoensin S, Madreiter-Sokolowski CT, Ramadani J, Waldeck-Weiermair M, Graier WF, Malli R. Application of genetically encoded fluorescent nitric oxide (NO) probes, the geNOps, for real-time imaging of NO signals in single cells. JOVE 2017.

Acknowledgements

As a PhD student I received funding from the Austrian Science Fund (FWF, P28529-B27 to Roland Malli) and by the Medical University of Graz through the PhD program Molecular Medicine (MOLMED).

Danksagung

An dieser Stelle möchte ich mich bei allen, die mir während der Arbeit an meiner Dissertation zur Seite gestanden sind, bedanken. Zuallererst will ich mich bei meiner Familie und meinen Freunden bedanken, die mir stets Rückhalt geben und mich auf meinem Lebensweg ermutigend begleiten.

Ich danke meinen lieben Kollegen für ihre Unterstützung bei der Durchführung von Experimenten, und den regen Austausch von Ideen und lebhafte Diskussionen, alles entscheidende Faktoren für die Entwicklung dieser Arbeit. Das freundschaftliche Miteinander im Laboralltag beflügelt und hilft, Rückschläge besser zu verkraften. Mein besonderer Dank gilt hier Christiane, Corina und Benjamin, mit denen ich einen Großteil des Weges gemeinsam gehen durfte.

Ich möchte mich bei René und Anna für die wertvolle Unterstützung im Bereich der Zellkultur bedanken, sowie bei Sonja und Markus für ihre Hilfsbereitschaft, die mir das Weiterkommen sehr erleichterten. Ein besondere Dank gilt auch meinen PhD-Kollegen in der „AG Malli“ Jeta, Helmut, Sandra und Emrah. Danke auch an Sasha, Sandra, Mercedes und Andreas für die gute Zusammenarbeit.

Für die wissenschaftliche Begleitung während meines PhD-Studiums danke ich den Mitgliedern meines Thesis-Komitees Wolfgang Graier und Helmut Bergler.

Und zuletzt gilt ein besonderer Dank meinem Supervisor Roland Malli, der mir die Möglichkeit gab, an einem so spannenden Projekt zu arbeiten, und mir den Weg zum PhD mit wertvollen Ratschlägen und Ideen ebnete.

Table of Contents

Abbreviations

Acetyl-CoA	Acetyl coenzyme A
ADP	Adenosine diphosphate
ALL	Acute lymphoblastic leukemia
AMP	Adenosine monophosphate
AMPK	AMP-activated protein kinase
ANT	Adenine nucleotide translocator
ATP	Adenosine triphosphate
CFP	Cyan fluorescent protein
Cyto	Cytosol
DMEM	Dulbecco's modified eagle's medium
ECAR	Extracellular acidification rate
ER	Endoplasmic reticulum
ETC	Electron transport chain
FAD	Flavin adenine dinucleotide
FP	Fluorescent protein
FRET	Förster Resonance Energy Transfer
GAPDH	Glyceraldehyde 3-phosphate dehydrogenase
GFP	Green fluorescent protein
GTP	Guanosine triphosphate
HK	Hexokinase
IMM	Inner mitochondrial membrane
MAM	Mitochondria-associated ER membranes
MEF	Mouse embryonic fibroblast

Mfn	Mitofusin
Mito	Mitochondria
mPTP	mitochondrial permeability transition pore
mTOR	mammalian target of rapamycin
MTR	MitoTracker Red FM
NAD/NADH	Nicotinamide adenine dinucleotide
NADP/NADPH	Nicotinamide adenine dinucleotide phosphate
NO	Nitric oxide
OCR	Oxygen consumption rate
OMM	Outer mitochondrial membrane
OXPHOS	Oxidative phosphorylation
P_i	Inorganic phosphate
PKM2	Pyruvate kinase isozyme M2
ROS	Reactive oxygen species
SEM	Standard error of the mean
SIM	Structured illumination microscopy
TCA cycle	Tricarboxylic acid cycle
TMRM	Tetramethylrhodamine methyl ester
TNBC	Triple negative breast cancer
TOM22	Translocase of the outer membrane 22
VDAC	Voltage-dependent anion channel
Wt	Wild-type
YFP	Yellow fluorescent protein

Zusammenfassung

Zahlreiche physiologische und pathophysiologische Vorgänge gehen mit Veränderungen im Energiemetabolismus von Zellen einher. Eine zentrale Rolle kommt hier ATP als Energieträger der Zelle zu. In dieser Arbeit wurden mithilfe genetisch kodierter Fluoreszenz-basierter ATP-Sensoren intrazelluläre ATP-Änderungen gemessen, mit dem Ziel, den Energiemetabolismus einzelner Zelle genauer zu beschreiben. Dabei stellte sich heraus, dass insbesondere mitochondrielle ATP-Spiegel starken Schwankungen unterliegen. So zeigte sich, dass HeLa-Zellen, die als Krebszellmodell dienten, ATP hauptsächlich über Glykolyse erzeugen, während ihre Mitochondrien ATP eher verbrauchen als produzieren. Andere Zelltypen, wie zum Beispiel Insulin produzierende Beta-Zellen (INS-1, MIN-6), generieren ATP hingegen überwiegend über oxidative Phosphorylierung in den Mitochondrien. Dementsprechend können mitochondrielle ATP-Messungen zur metabolischen Charakterisierung verschiedener Zelltypen genutzt werden, wie es in dieser Arbeit für eine Reihe von Krebszelllinien (H1299, A548, Calu-3, SkBr3, MCF7, MDA-MB231, SH-SY5Y) sowie Wildtyp und Mfn2 Knockout MEFs gezeigt wurde. Zudem erwiesen sich ATP-Messungen als geeignete Methode zur Aufklärung mechanistischer Vorgänge im Zusammenhang mit ATP-Produktion und Transport. So wurde in HeLa-Zellen nachgewiesen, dass mitochondriell lokalisierte Hexokinasen den initialen Schritt der Glykolyse an den mitochondriellen ATP-Pool koppeln. Damit demonstriert diese Arbeit nicht nur die Tragweite mitochondrieller ATP-Messungen zur metabolischen Charakterisierung von Zellen und Zellpopulationen, sondern liefert auch neue Erkenntnisse in Bezug auf Umsatz und Verteilung von ATP in der Zelle.

Abstract

Many physiological and pathophysiological processes are accompanied by alterations in the energy metabolism of a cell. Such changes particularly affect ATP generating pathways. In this work genetically encoded fluorescent ATP sensors were used to measure ATP dynamics on the level of individual cell. Mitochondrial ATP levels were found to be most dynamic, with cell-type specific features. HeLa cells, as a model for cancer cells, produce ATP predominantly via aerobic glycolysis, while their mitochondria tend to consume ATP rather than generate it via oxidative phosphorylation. Insulin producing beta cells (INS1, MIN-6), on the other hand, mainly rely on mitochondrial ATP production via oxidative phosphorylation. These results demonstrate, that mitochondrial ATP measurements can be used for the metabolic characterization of different cell types, as it was done in this study for different cancer (H1299, A548, Calu-3, SkBr3, MCF7, MDA-MB231, SH-SY5Y) and non-cancer (wild-type and Mfn2 knockout MEFs) cells. Furthermore, mitochondrial ATP measurements in HeLa cells revealed a tight coupling of the mitochondrial ATP pool with mitochondria-associated hexokinase enzymes. Altogether, the findings presented in this work add new perspectives on cellular bioenergetics and demonstrate that live-cell imaging of mitochondrial ATP dynamics is a powerful tool to evaluate the metabolic flexibility and heterogeneity of cells and cell populations.

1. Introduction

A fundamental question in cell biology is how cells create, store and consume energy. Thanks to the constant effort of many scientists, our understanding of the cell's bioenergetics has grown considerably over the last decades. But there still remain plenty of open questions, unconfirmed hypotheses, and contentious issues. Many of such much-debated topics bear upon the abnormal energy metabolism of cancer cells. Pioneering work on cancer cell metabolism was done by Otto Warburg already in the 1920s, and his observations, that cancer cells produce ATP predominantly by high rates of (aerobic) glycolysis, became known as the "Warburg effect" (1–4). The perception that a high glycolytic rate is typical and important for cancer cells continues to this day and has a major impact on basic research on cancer. However, we still lack understanding of the mechanisms behind the Warburg effect, and major questions have not been addressed sufficiently, such as: *What is the origin of the metabolic changes during cancerogenesis and how do cells cope with such drastic physiological changes as the "Warburg effect"?*

This work aims to extend our knowledge in this field, by taking advantage of new technological possibilities, which allow us to approach certain problems from a different angle. Namely, I used genetically encoded fluorescent biosensors to measure fluxes of intracellular metabolites, in particular ATP, in living cancer and non-cancer cells, to gain insights into their metabolic activity. The following introduction gives an overview of the cellular energy metabolism, with a focus on cancer cell metabolism, followed by a concise introduction to genetically encoded biosensors, with a focus on ATP sensors used in this study.

1.1. Cellular energy metabolism

The following introduction shall provide background knowledge on specific topics of cellular energy metabolism to facilitate the understanding of the results and interpretations presented in this thesis.

1.1.1. Carbohydrate metabolism

Carbohydrate metabolism involves various metabolic pathways (5). First and foremost, the breakdown of carbohydrates, in particular glucose, serves energy production in the form of ATP. For that purpose, glucose is converted to two molecules of pyruvate during glycolysis, which results in the net production of two molecules of each ATP and NADH. The first five reactions of glycolysis constitute the so called "investment phase", as ATP is consumed to convert glucose into three-carbon sugar phosphates (glyceraldehyde 3-phosphate). The next five steps of glycolysis then serve ATP generation and are therefore collectively referred to as "pay-off phase". Following glycolysis, pyruvate is transported into mitochondria and decarboxylated to acetyl-CoA. Acetyl-CoA enters the TCA cycle, where it is oxidized to CO_2 and H_2O. One cycle round yields three molecules of NADH, one $FADH_2$, and one GTP (or ATP). NADH and $FADH_2$ serve as electron donors for oxidative phosphorylation. The transfer of electrons via the complexes of the respiratory chain with O_2 as the final acceptor provides the energy required to build a proton gradient across the inner mitochondrial membrane (6). The energy stored in form of the proton gradient drives the ATP synthase to generate ATP from ADP and inorganic phosphate (P_i) (7,8).

The first step of glycolysis is the phosphorylation of glucose to glucose 6-phosphate by hexokinase enzymes (9,10). Beside glycolysis, glucose 6-phosphate, as a central metabolite, can also be directed to the pentose phosphate pathway or glycogenesis (5). In contrast to glycolysis, which primarily serves energy production, the pentose phosphate pathway provides NADPH as reducing equivalent for biosynthetic reactions, and other intermediates for anabolic pathways, such as ribose 5-phosphate for nucleotide biosynthesis. The pentose phosphate pathway is most active in the liver, kidney, brain, testes, and erythrocytes, albeit the required enzymes are present in most cells. Glycogenesis, on the other side, takes place in liver and muscle cells and allows the storage of glucose in the form of glycogen (glycogenesis). In turn, glycogen can be converted to glucose 6-phosphate during glycogenolysis, which again takes place in liver and muscle cells. In muscle cells, glucose 6-phosphate enters glycolysis for ATP production. In liver and kidney cells, on the other hand, glucose 6-phosphatase allows converting glucose 6-phosphate into glucose, which is released into the bloodstream where it can be taken up by other cells. Glucose can also be

generated from different non-carbohydrate carbons via gluconeogenesis, which also takes place in liver and kidney.

1.1.2. Metabolic flexibility

The concept of metabolic flexibility gained popularity in obesity and type 2 diabetes research (11). Here, metabolic flexibility mainly refers to fuel selection (fatty acid oxidation, glucose oxidation) in muscle and adipose cells during fasting and feeding conditions, in response to exercise or under similar conditions, relevant in this field. While healthy cells are considered to be metabolically flexible, metabolic inflexibility in associated with pathophysiology.

However, a certain metabolic flexibility is essential for many cells, in order to adjust to changing conditions (11,12). Macrophages, for examples, are able to adapt their metabolism, depending on different activation states (13). Similar to cancer cells, inflammatory macrophages have a high glycolytic activity and low OXPHOS. Here, the upregulation of glycolysis is considered to serve ATP production at high rates, required for the phagocytic and secretory functions of macrophages. Moreover, glycolysis fuels the pentose phosphate pathway, in order to support the synthesis of amino acids, nucleotides, and NADPH as co-factor for ROS and NO production.

1.1.3. Metabolic alterations in cancer

Metabolic reprogramming is a common feature of cancer cells. Both, the activation of several oncogenes and the loss of tumor suppressors have been found to support metabolic reprogramming of cells, which thereby acquire metabolic flexibility and specific metabolic settings that promote their survival and growth. However, it has been suggested that cancer might be rather a metabolic than a genetic disease (14), meaning metabolic alterations and not DNA mutations initiate tumorigenesis.

Ensuing from the pioneering work of Otto Warburg and others, the metabolic aspects of cancer have been extensively investigated over the last century, and metabolic alterations are now considered as one of the hallmarks of cancer (15,16). Many scientists concentrate

their efforts on understanding the origin and functions of metabolic reprogramming in cancer. Here I will summarize some basic considerations on cancer cell metabolism, for more information a range of comprehensive reviews is available (17–19).

The best known and most common metabolic feature of cancer cells is the so called "Warburg effect" (1). In most mammalian cells glycolysis is repressed by oxygen ("Pasteur effect"). Some proliferating cell types, and in particular many cancer cells, however, continue to have high rates of glycolysis, also in the presence of oxygen. This phenomenon is known as "aerobic glycolysis" or "Warburg effect". Already in the 1920s, Otto Warburg observed that cancer tissue is highly glycolytic and produces lactate from pyruvate (1–4,20). Although aerobic glycolysis is less efficient in producing ATP than oxidative phosphorylation, it seems to be the preferred metabolic pathway of cancer and other rapidly proliferating cells (21,22). Yet, there is no common sense about the origin and benefits of the high glycolytic activities in these cells (1,21,23).

Initially, Warburg and others thought that mitochondrial function was impaired in cancer cells and that the high glycolytic activity resulted thereof as a compensatory mechanism (3). This explanation proved wrong though, as mitochondria are functioning in most cancer cells, and, in some cancers, also essentially contribute to ATP production (24,25).

ATP production via glycolysis is faster than by oxidative phosphorylation, provided there is a steady supply with glucose (26). Thus, cancer cells might gain a selective advantage over normal cells by their high glycolytic activity. Furthermore, a high glycolytic rate could provide glycolytic intermediates for biosynthetic pathways (21), which is required in growing cells. Aerobic glycolysis is also considered as an adaptation mechanism to hypoxia, which develops in pre-malignant lesions (23).

However, there are also other fuels beside glucose which are preferably used by cancer cells for energy and biomass generation. A prominent example is glutamine, which is involved in bioenergetics, oxidative stress protection and biosynthetic pathways as a source for carbon and nitrogen (27–29). For ATP production glutamine can be converted to α-ketoglutarate (via glutamate), which enters the TCA cycle, where NADH and $FADH_2$ are produced to be used as electron donors for the electron transport chain (ETC) and ATP production via

mitochondrial respiration. Also in the absence of respiratory chain activity ATP can be generated via the TCA cycle by the succinate-CoA ligase reaction.

Considering the peculiarities of cancer cell bioenergetics, it is certainly of great importance to have a closer look on ATP dynamics in cancer cells. One important tool, allowing to monitor ATP in living cells, are genetically encoded fluorescent ATP sensor, which will be explained in the following chapter.

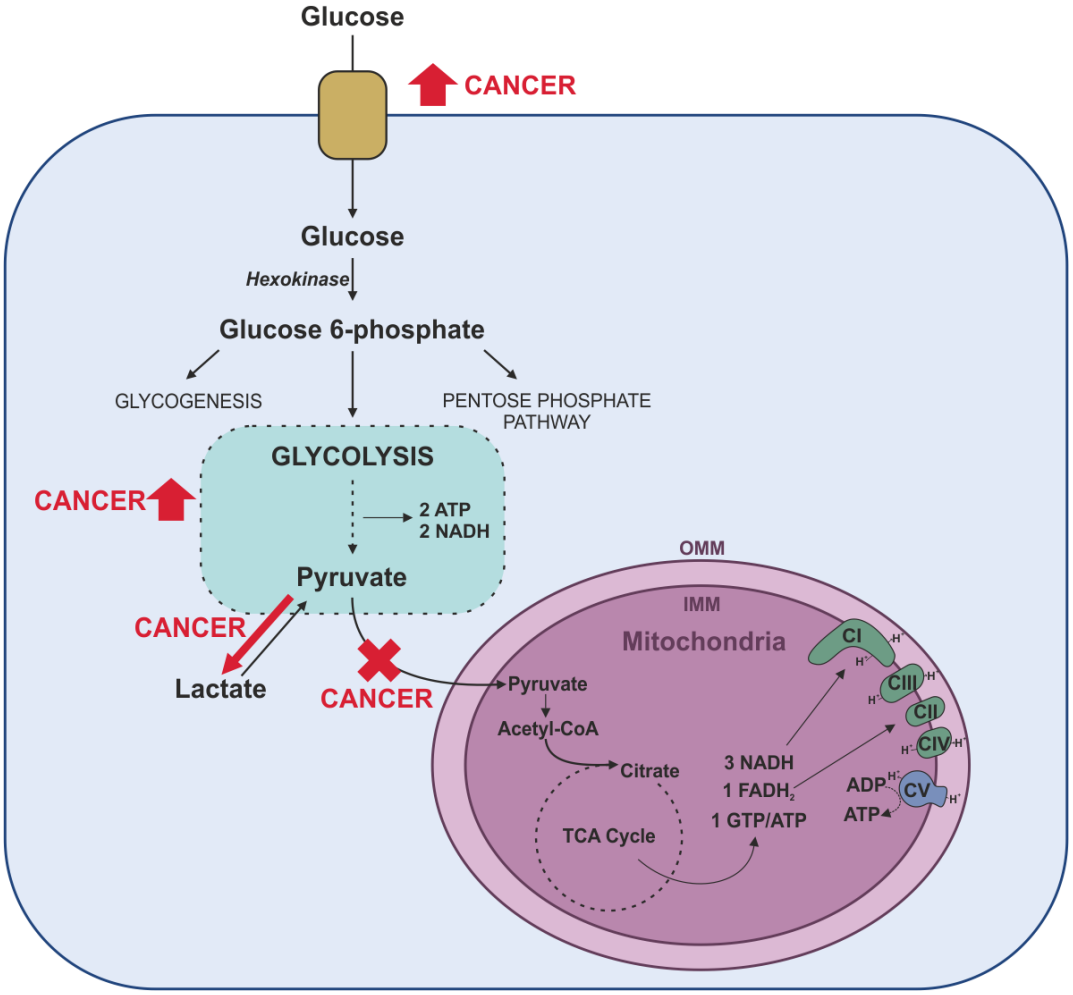

Figure 1.1. Glucose metabolism at a glance. Glucose is the main energy fuel for cells. After its uptake, glucose is phosphorylated to glucose 6-phosphate. Glucose 6-phosphate can enter the pentose phosphate pathway to generate NADPH for anabolic reactions, glycogenesis for energy storage or glycolysis for energy production. The glycolytic degradation of glucose to pyruvate yields a net production of two ATP and two NADH molecules. Pyruvate is imported into mitochondria to enter the TCA cycle and OXPHOS for ATP production. Cancer cells, however, have only low rates of mitochondrial respiration, and produce ATP primarily via high rates of glycolysis, followed by lactic acid fermentation. Therefore, also glucose uptake is strongly increased in cancer cells.

1.1.4. Mitochondrial metabolism and cancer

In light of the fact that most cancer cells choose aerobic glycolysis over oxidative phosphorylation for ATP production, the role of mitochondria in cancer has been neglected for many years. However, today's prevailing view is that mitochondria are important players in cancer development. Alterations in mitochondrial functions, including bioenergetics and metabolism as well as mitochondrial biogenesis, mitophagy, mitochondrial dynamics (fusion and fission) and oxidative stress, are linked to tumorigenesis (30–33). I will now briefly discuss selected functions of mitochondrial metabolism in cancer cells.

One major aspect which distinguishes cancer from non-cancer cells is how they utilize the glycolytic end-product pyruvate. As already mentioned, cancer cells do not oxidize pyruvate within mitochondria, which is also reflected in the downregulation or deletion of the mitochondrial pyruvate carrier (34). Furthermore, many tumors upregulate a specific isoform of the pyruvate kinase with low activity, namely PKM2, which favors the accumulation of glycolytic intermediates that are required to fuel biosynthetic pathways (e.g. pentose phosphate pathway) in fast growing cancer cells (35).

Mitochondria are also essential for the utilization of glutamine by cancer cells. As mentioned before, glutaminolysis, that is glutamine oxidation, may serve energy production in mitochondria. This phenomenon is often connected with the upregulation of glutaminase, which converts glutamine to glutamate (36). On the other hand, cancer cells also use glutamine for biosynthetic purposes via the reversal of TCA cycle reactions (37,38). Same as glutamine, aspartate is required for protein and nucleotide synthesis. In contrast to glutamine, however, aspartate cannot be taken up from the circulation in sufficient amounts, and therefore cells, and especially highly proliferative cancer cells, rely on aspartate synthesis, which occurs by the transamination of oxaloacetate to glutamate, which takes place in the cytosol by GOT1 as well as within mitochondria by GOT2 (32).

Intriguingly, several enzymes of the TCA cycle have recently been found to be deregulated or mutated in cancer cells (39). Moreover, many cancers contain mitochondrial DNA mutations. These mutations mainly affect respiratory chain complexes, resulting in defective mitochondrial bioenergetics (39,40). Most cancer-associated mutations in the mitochondrial DNA concern complex I of the respiratory chain, thereby affecting bioenergetics as well as

redox homeostasis in cancer cells. Accordingly, increased ROS levels are observed in many cancers, as a consequence of ETC mutations in combination with oncogenic signaling and a hypoxic environment (30). On the one hand, increased ROS levels are considered a natural consequence of cancer-associated metabolic reprogramming. On the other hand, enhanced ROS signaling was found to promote tumor survival, while antioxidant activity is elevated in order to prevent ROS-mediated cytotoxicity (41).

Altogether, mitochondria are essentially involved in the metabolic rewiring of cancer cells. The better understanding of the metabolic role of mitochondria in cancer cells will help to comprehend cancer development and may reveal new therapeutic targets. By analyzing mitochondrial ATP fluxes in cancer cells, this thesis should contribute towards achieving this goal, by the use of real-time imaging of subcellular ATP dynamics in various cancer cell types (42).

1.2. Genetically encoded fluorescent biosensors

The development of a wide range of fluorescent sensors has empowered us to observe cellular processes in living cells almost in real-time. The two main categories of fluorescent sensors comprise so-called chemosensors (43,44) and genetically encoded sensors (45). Chemosensors include for example the intracellular Ca^{2+} indicator Fura-2AM or the mitochondrial membrane potential dyes TMRM and JC-1 (46), as well as ROS (47) or NO indicators (48,49), and many more. In addition, there is a wide range of genetically encoded biosensors available, which enable us to measure intracellular metabolites such as glucose (50), ATP (51–56), NADH (57–59), or NO (60–62), as well as ions, e.g. Ca^{2+} (63,64) or K^{+} (65), intracellular pH (66–69) and ROS (47,70). Moreover, it is also possible to use such sensors to monitor the activity of certain enzymes, e.g. AMPK (71) or caspase (72,73), or cell cycle progression (74,75).

1.2.1. Functional principle of genetically encoded fluorescent biosensors

Genetically encoded fluorescent biosensors generally consist of one or more fluorescent proteins (FP) and in most cases a sensor domain (45). The binding of a specific molecule, such as ATP or Ca^{2+}, to the sensor domain changes the fluorescent properties of the probe. Most common are among others single FP and Förster Resonance Energy Transfer (FRET)-based sensors. In the case of single FP sensors, only one FP is used as a readout. The FP itself may have the intrinsic capability to change its fluorescent properties depending on the concentration of an analyte. Among these probes are in particular pH probes, such as SypHer (66). Single FPs may be also be fused do a sensor domain, such as in the case of Pericam and GCaMP Ca^{2+} probes (76,77). The interaction of the analyte with the sensor domain affects the fluorescence of the FP by various possible mechanisms. FRET-based sensors, on the other hand, consist of a so-called FRET pair of two spectrally overlapping fluorescent proteins and a sensor domain, usually fused in between the two FPs. Between the two FPs energy is transferred via FRET from the excited donor (e.g. CFP) to the acceptor (e.g. YFP) (78,79). In sensor design, the FRET principle has proven versatile in combination with an expansive set of possible sensor domains provided by nature. Moreover, FRET sensors have the major advantage of being ratiometric. In contrast, most – but not all – single FP probes are only intensiometric, which means they can only measure relative changes. However, single FP probes outclass FRET sensors as regards that they are smaller and have a narrower spectral bandwidth, which is favorable for simultaneous measurements with multiple fluorescent sensors.

All genetically encoded fluorescent biosensors can theoretically be targeted to different subcellular compartments such as mitochondria, the ER or the nucleus by adding respective localization sequences. In most cases, the targeting of the probe is applicable also in practice. Moreover, the pallet of biosensors is destined to keep on growing by interchanging fluorescent proteins or by mutating the sensor domain. The latter is used to produce sensor variants with different affinities for their ligand, which expands the applicability of the probe in different (physiological) environments.

In this work, I made use of such genetically encoded fluorescent sensors, in particular the ATP probe AT1.03 (51), for assessing metabolic dynamics in living cells.

1.2.2. ATeam ATP biosensors

In 2009, Imamura and colleagues developed the first biosensors for real-time monitoring of intracellular ATP levels in living cells, the so called ATeams (51). The FRET-based probe is composed of a cyan and a yellow fluorescent protein, flanking the ε subunit of the *Bacillus subtilis* F_1F_o ATP synthase. The latter functions as ATP sensor domain; ATP binding induces a conformational rearrangement of the domain, which brings the two fluorescent proteins into close proximity, allowing FRET from CFP to YFP. For measuring ATP, the probe is excited at 430 nm (CFP excitation wavelength) and both, CFP and YFP emissions are detected. The YFP to CFP intensity ratio increases with growing ATP concentrations. Imamura and colleagues also constructed variants targeted to the nucleus and mitochondria (51). For nuclear localization, three copies of the respective signal sequence of the SV40 large T-antigen were fused to the N terminus of AT1.03, while mitochondrial targeting was achieved by the addition of a duplex of the cytochrome c oxidase subunit VIII signal sequence. In addition, Vishnu et al. (52) targeted the sensor also to the ER by adding the calreticulin signal sequence at the N terminus, and the ER retention signal KDEL at the C terminus. In this work, AT1.03, mtAT1.03, and ERAT1.03 were used to measure ATP in the cytosol, mitochondria and ER, respectively.

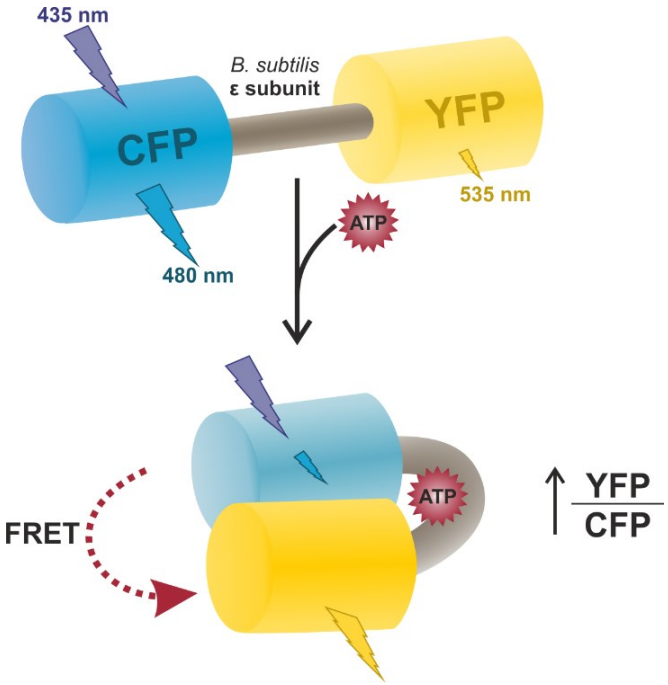

Figure 1.2. Basic design of ATeam ATP biosensors. ATeams were invented by Imamura et al. (51). They are composed of a YFP and CFP protein flanking the ε subunit of the *B. subtilis* ATP synthase as sensor domain. The probe is excited at 435 nm, emission is collected at 480 nm (CFP) and 535 nm (YFP). Binding of ATP to the sensor domain induces a conformational rearrangement of the probe, resulting in enhanced FRET from CFP to YFP. The YFP/CFP ratio thus increases with growing ATP levels.

1.3. Aims of this study

This study aims to characterize and analyze the energy metabolism of different cell types, with the focus on cancer cells. In particular, intracellular ATP dynamics will be monitored under various conditions with the help of genetically encoded fluorescent ATP sensors. Although live-cell imaging of ATP was introduced already ten years ago (51,54), the high potential of this approach for studying cellular bioenergetics has not been fully exploited yet. In contrast to conventional biochemical methods, which mostly require cell lysis, imaging of metabolites allows to investigate metabolic processes in intact cells under more physiological conditions. Furthermore, the imaging approach permits to resolve differences between single cells, which cannot be seen with most classical biochemical methods which use cell populations. Since most cancer cells have an altered energy metabolism compared to their non-transformed counterparts, it is required to learn more about their metabolic peculiarities. As described above, cancer cells rely mainly on glycolysis for ATP production. Therefore, the first goal of this work will be to analyze how HeLa cells, a widely used cancer cell line, respond to the removal of their main energy source glucose from the media. The primary question will be how the absence of glucose affects ATP levels on the subcellular level, specifically in the cytosol, mitochondria and ER. Based on the results from HeLa cells, ATP-imaging will be applied for metabolic analyses of other cancer and non-cancer cells. Overall, this thesis should establish ATP measurements as a versatile tool to investigate various aspects of the cellular energy metabolism.

2. Material and Methods

The experimental details of this study were published in a similar manner in my first-author publication (42).

2.1. Cells and cell culture media

HeLa S3, H1299, and SH-SY5Y cells come from ATCC; MIN-6, MDA-MB231, MCF7, SkBr3, Calu-3 and A549 cells from the Core Facility Alternative Biomodels and Preclinical Imaging, Medical University of Graz (Graz, Austria). INS-1 cells were obtained from C.B. Newgard, Department of Pharmacology and Cancer Biology, Duke University School of Medicine, USA. Mouse embryonic fibroblasts (MEFs) were a gift from Thomas Simmen, Department of Cell Biology, University of Alberta, Canada.

HeLa, MCF7, MDA-MB231, SkBr3, H1299 and MEF cells were grown in Dulbecco's modified eagle's medium (DMEM) containing 10% FCS, 100 U/mL penicillin, 100 µg/mL streptomycin, 2.5 µg/mL amphotericin B, and 2 mM glutamine. A549, Calu-3, and SH-SY5Y cells were cultivated in a 1:1 mixture of Ham's F12 medium and DMEM supplemented with 10% fetal bovine serum, 100 U/mL penicillin, 100 µg/mL streptomycin, 2.5 µg/mL amphotericin B and 2 mM glutamine. INS-1 cells were grown in GIBCO RPMI medium 1640 supplemented with 10% FCS. MIN-6 cells were cultured in Dulbecco's modified eagle's medium (DMEM) supplemented with 25 mM D-glucose, 10 mM HEPES, 10% FCS, 1 mM sodium pyruvate, 50 µM β-mercaptoethanol, 100 U/mL penicillin and 100 µg/mL streptomycin. Cell culture substances were obtained from Life Technologies (Vienna, Austria) and Carl Roth (Karlsruhe, Germany). All cells were grown at 37°C with 5% CO_2.

2.2. Transfection

For the experiments, cells were seeded in 6-well plates with (for microscopy) or without (RNA isolation) 30 mm imaging dishes. They were transiently transfected at a confluence of 60 to 70% one to two days before the measurement. The transfection mix contained (per

well): 1 mL DMEM (without serum and antibiotics), 2.5 µL TransFast transfection reagent (Promega, Madison, WI, USA) and 1.5 µg plasmid DNA encoding the respective fluorescent sensor and/or 100 nM siRNA. The transfection mix was replaced with full culture medium 6 to 12 hours after transfection. The siRNAs against hexokinase 1 and hexokinase 2 were obtained from Santa Cruz Biotechnology (Heidelberg, Germany). The siRNAs are pools of three target-specific 19 nucleotide siRNAs. Control siRNA was obtained from Microsynth (Balgach, Switzerland).

ATP sensors were a gift from Hiromi Imamura, Kyoto University, Kyodai Graduate School of Biostudies, Japan (51). FLHKI-pGFPN3 and FLHKII-pGFPN3 were a gift from Hossein Ardehali (Addgene plasmid # 21917 and # 21920) (80). pcDNA3.1 FLII^{12}Pglu-700µδ6 was a gift from Wolf Frommer (Addgene plasmid # 17866) (50). SypHer and SypHer mt were a gift from Nicolas Demaurex (Addgene plasmid # 48250 and # 48251) (66).

2.3. Microscopy

For all imaging experiments, cells were equilibrated in loading buffer for one hour. Loading buffer contained: 2 mM $CaCl_2$, 138 mM NaCl, 5 mM KCl, 1 mM $MgCl_2$, 10 mM D-glucose, 2 mM L-glutamine, 10 mM HEPES, 2.6 mM $NaHCO_3$, 0.44 mM KH_2PO_4, 0.34 mM Na_2HPO_4, 0.1% vitamins, 0.2% essential amino acids, 1% penicillin-streptomycin, pH adjusted to 7.4 with NaOH. All experiments were performed at room temperature in ambient atmosphere. For life cell imaging experiments, cells were placed in a flow chamber. A gravity-based perfusion system (NGFI, Graz, Austria) in combination with a vacuum pump (Chemistry diaphragm pump ME 1c, Vacuubrand, Wertheim, Germany) allowed the steady perfusion of the cells with fresh buffer and the switching between different buffers. Standard physiological buffer contained: 2 mM $CaCl_2$, 138 mM NaCl, 5 mM KCl, 1 mM $MgCl_2$, 10 mM D-glucose, 10 mM HEPES, pH adjusted to 7.4 with NaOH. For glucose free conditions, 10 mM D-mannitol (Sigma Aldrich, Vienna, Austria) was added instead of glucose. If required, glucose was replaced by 2-deoxy-D-glucose (2-DG, Alfa Aesar, ThermoFisher, Karlsruhe, Germany) or D-mannose (Carl Roth, Karlsruhe, Germany). Oligomycin and antimycin A were dissolved from 10 mM stock solutions (in DMSO). Oligomycin was

obtained from Tocris (Bristol, UK) or Sigma Aldrich (Vienna, Austria), antimycin A was from Sigma Aldrich (Vienna, Austria). Other chemicals were from Carl Roth (Karlsruhe, Germany).

Cells were selected randomly for the measurement, the total numbers of cells measured for each experiment are indicated in the figure legends. The measurements were performed with an iMic inverted and advanced fluorescent microscope using a x40 magnification objective (alpha Plan Fluor x40, Zeiss, Göttingen, Germany) with a motorized sample stage (TILL Photonics, Graefling, Germany). For control and acquisition, the software Live Acquisition 2 (TILL Photonics) was used. CFP/YFP FRET sensors were excited at a wavelength of 430 nm; emission was collected simultaneously at 535 and 480 nm using an optical beam-splitter (Dichroic 69008-ET-ECFP/EYFP/mCherry). Data processing was performed with the Offline Analysis application (TILL Photonics).

The SIM-setup is composed of a 405 nm, 488 nm, 515 nm, 532 nm and a 561 nm excitation laser introduced at the back focal plane inside the SIM-box with a multimodal optical fiber. For super-resolution, a CFI SR Apochromat TIRF 100x-oil (NA 1.49) objective was mounted on a Nikon-Structured Illumination Microscopy (N-SIM®) System with standard wide field and SIM filter sets and equipped with two Andor iXon3® EMCCD camera mounted to a Two Camera Imaging Adapter (Nikon Austria, Vienna, Austria). Cells were incubated for 40 min with Mitotracker Red-FM in loading buffer prior to imaging and washed twice with loading buffer. GFP was excited at 488 nm, MitoTracker Red was excited at 561 nm. For calibration and reconstruction of SIM images, the Nikon software Nis-Elements was used. To align both channels for parallel dual color experiments NIS-Elements Two-CAM registration was used taking the TetraSpeck bead samples. Image analysis was done using a custom-made ImageJ macro. Cells were selected by hand within the SIM images. Images were background corrected with an ImageJ Plugin (Mosaic Suite, background subtractor, NIH). The colocalization coefficients Pearson and Manders 1 and 2 were determined on a single cell basis with the ImageJ coloc 2 tool. Channel 1 represents the GFP and channel 2 the mCherry label. While the Pearson coefficient was determined with not thresholded data, the Manders 1 and 2 coefficients were determined on the basis of Costes thresholded images.

2.4.mRNA isolation and qRT-PCR

For qRT-PCR total RNA was isolated with a total RNA isolation kit (Peqlab, Erlangen, Germany). For reverse transcription a cDNA synthesis kit (Applied Biosystems, Foster City, CA) was used. For qRT-PCR the QuantiFast SYBR Green RT-PCR kit (Qiagen, Hilden, Germany) was used. Relative gene expression was normalized to human GAPDH (QuantiTect; Qiagen). The reaction was performed on a LightCycler 480 (Roche Diagnostics, Vienna, Austria). Primers were obtained from Invitrogen (Vienna, Austria); their sequences were as follows (5'-3'): HK1-forward GACTCGCTTCAG-GAAGGAGATG, HK1-reverse ACATCTTGACTGTGGCTGTTGG, HK2-forward GATTGTCCGTAACATTCTCATCGA, HK2-reverse TGTCTTGAGCCGCTCTGAGAT.

2.5.Measurement of mitochondrial respiration

One day before the experiment cells were plated on XF96 polystyrene cell culture microplates (Seahorse®, Agilent, CA, USA). They had to be 100% confluent on the day of the experiment. Before the measurement cells were washed and incubated in XF assay medium supplemented with 1 mM sodium pyruvate, 2 mM glutamine and 5.5 mM D-glucose. An XF96 extracellular flux analyzer was used to measurer oxygen consumption rate (OCR) and extracellular acidification rate (ECAR). OCR (pmol O_2/min) and ECAR (mpH/min) values were normalized to protein content.

2.6.Data analysis

For data analysis Microsoft Excel (Redmond, WA, USA) and GraphPad Prism5 (GraphPad Software Inc.) were used. For both the YFP and CFP intensities, the respective background signals were subtracted. Then the YFP/CFP ratio was calculated. In case of live-cell imaging data, curve fitting was used to correct for bleaching. Representative ratio images were created using MetaMorph microscopy automation and image analysis software (Molecular Devices, Sunnyvale, CA, USA). Statistical analysis was performed with GraphPad Prism5 using either unpaired Student's t-test or one-way ANOVA with Tukey's Multiple

Comparison Test. N represents the number of independent experiments (at least three); the total number of measured cells is also indicated.

3. Results

Most of the results presented in this work are part of my first-author publication (42).

In the first part of this section I will describe how glucose removal affects intracellular ATP levels and other metabolic parameters in HeLa cells as a cancer cell model. Based on the results with HeLa cells, ATP measurements were then used for the metabolic profiling of other cells, which will be specified in the second part of the results section.

3.1. Part1 – Effects of glucose withdrawal on ATP and other metabolic parameters in HeLa cells

Since most cancer cells produce ATP primarily via high rates of glycolysis, this study aimed to evaluate the immediate effects of glucose removal on intracellular ATP levels in HeLa cells. Furthermore, intracellular glucose and NADH levels as well as the cytosolic and mitochondrial pH were measured, in order to better understand the destiny of glucose within this cancer cell line.

3.1.1. Acute glucose starvation causes intracellular ATP depletion with organelle specific kinetics

To monitor intracellular ATP levels, HeLa cells were transfected with FRET-based ATP sensors targeted to the cytosol (AT1.03), mitochondria (mtAT1.03) or endoplasmic reticulum (ERAT1.03) (51,52,56). During the experiments cells were selected depending on the expression and the proper localization of the respective ATP probes (**Figure 3.1A**) (42). ATP levels were traced in single cells by measuring FRET ratio signals of the respective sensors over time. In untreated cells, ATP levels were the highest in the cytosol, a little lower in the mitochondrial matrix and the lowest in the ER (**Figure 3.1A-C**) (42). Next, the main fuel for ATP production – glucose – was removed from the cells by switching to a glucose free buffer, to analyze the cellular ATP turnover rate and how the different organelles were affected (42). In mitochondria, ATP levels first slightly increased before they rapidly dropped, resulting in a characteristic peak signal (**Figure 3.1B**). After glucose re-addition, mitochondrial ATP levels recovered quickly (**Figure 3.1A,B**). Cytosolic and ER ATP levels

on the other hand decreased continuously and slowly, and did not recover completely (**Figure 3.1A,B**).

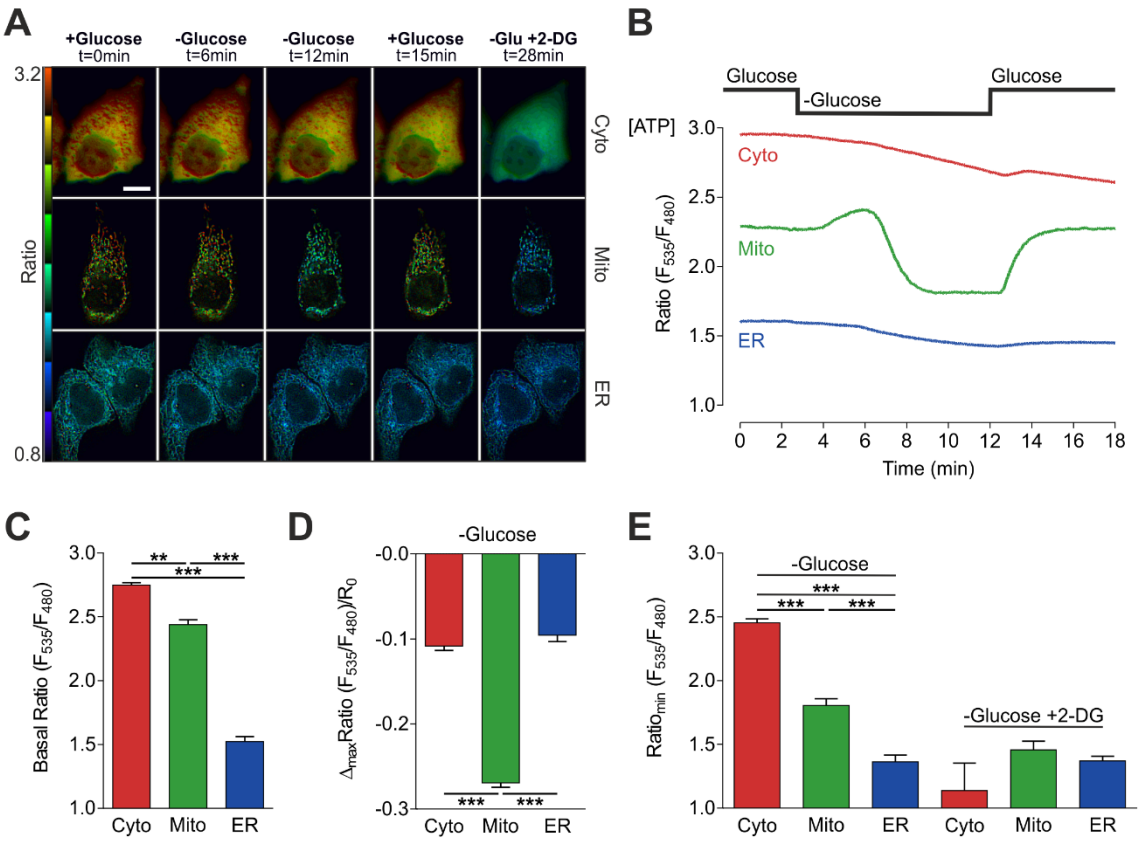

Figure 3.1. Acute glucose starvation causes strong ATP changes within mitochondria of HeLa cells. (A) Representative FRET ratio images of cytosolic, mitochondrial and ER-targeted ATP probes (ATeams) under basal conditions and at different time points after glucose depletion and subsequent 2-DG treatment in the absence of glucose. Scale bar represents 20 µm. **(B)** Representative single cell responses to glucose deprivation of FRET ratio signals of cells expressing cytosolic (red), mitochondrial (green) or ER-targeted (blue) ATeams. **(C)** Basal FRET ratio values (mean, SEM) in the cytosol (red column, N=5/42 cells), mitochondria (green column, N=24/124 cells) and ER (blue column, N=7/27 cells). ** $p < 0.01$, *** $p < 0.001$. **(D)** Maximal changes (mean, SEM) of normalized FRET ratio signals in response to glucose removal (10 mM to 0 mM). *** $p < 0.001$. **(E)** Minimal FRET ratio values after glucose depletion (*left columns*) and upon addition of 10 mM 2-DG in the absence of glucose (*right columns*) in cells expressing cytosolic (red columns, N=3/25 cells), mitochondrial (green columns, N=7/31 cells) or ER-targeted (blue columns, N=7/31 cells) ATP probes. Mean, SEM, *** $p < 0.001$. [Figure reproduced from Depaoli et al., Cell Reports 2018.]

In repeated measurements of mitochondrial ATP in different passages of HeLa cells, the response of mitochondrial ATP to glucose withdrawal had the same characteristic features, which are the peak signal and the fast depletion and recovery (**Figure 3.2A**). Furthermore, in some measurements mitochondrial ATP levels first slightly dropped before they increased. However, in detail the time courses were rather variable, not only depending on the passage number, but also in different cells of one dish. The greatest heterogeneity was related to the peak height and width. Also the maximal reduction of mitochondrial ATP was rather different from cell to cell, while the kinetics of the ATP drop and recovery were more consistent.

If glucose was substituted with its analogue 2-deoxyglucose (2-DG), mitochondrial ATP levels responded very differently than in the absence of any hexose sugar (**Figure3.2B**) (42). There was no transient increase of the mitochondrial ATP signal and the mitochondrial ATP depletion was faster and more pronounced (**Figure 3.2B,D**). Like glucose, 2-DG is phosphorylated by hexokinase enzymes which catalyze the first step of glycolysis; however, it cannot be utilized in the following steps of glycolysis, and hence no ATP can be produced from 2-DG.

Same as 2-DG, the glucose epimer mannose is also phosphorylated by hexokinases. Mannose is turned to mannose 6-phosphate, which is then transformed to fructose 6-phosphate by mannose 6-phosphate isomerase. Fructose 6-phosphate can now enter the glycolytic pathway. Based on this information, the switch from glucose to mannose should not considerably affect mitochondrial ATP levels. Yet mitochondrial ATP levels rapidly declined with similar kinetics as upon glucose removal without substitution (**Figure 3.2C**) (42). However, there was no transient increase of mitochondrial ATP if glucose was replaced with mannose, and mitochondrial ATP levels started to drop earlier than in the absence of any hexose (**Figure 3.2C**). The strong mitochondrial ATP depletion in the presence of mannose (**Figure 3.2C,D**) indicates that mannose cannot be used for ATP generation during glycolysis.

If glucose was substituted with either 2-DG or mannose, mitochondrial ATP depletion was more pronounced than in the absence of any hexose (**Figure 3.2D**). This can be explained by expenditure of ATP for the phosphorylation of 2-DG or mannose.

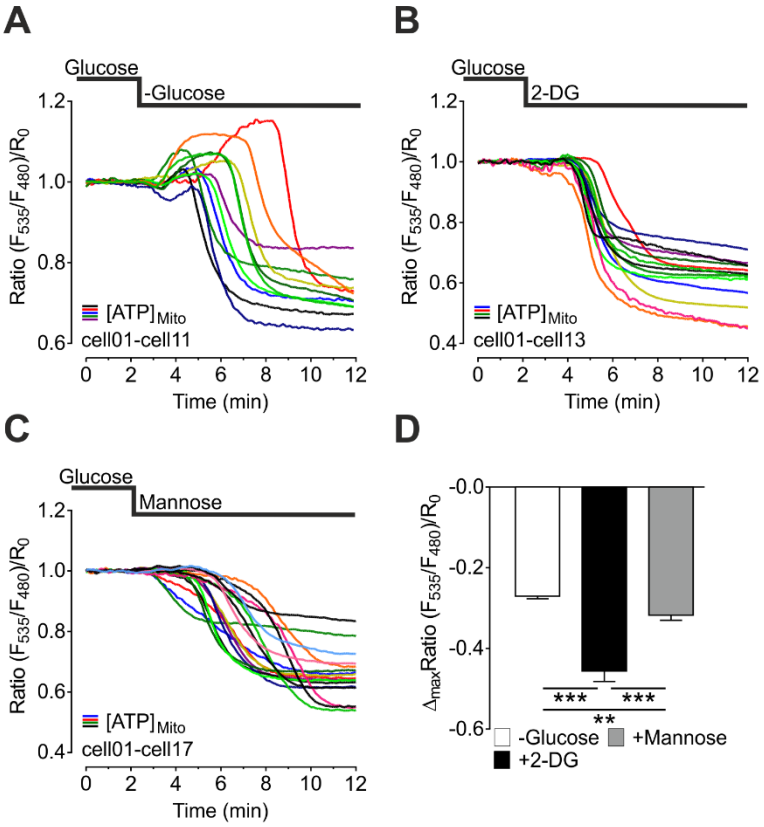

Figure 3.2. Mitochondrial ATP elevations are prevented by glucose substitution with other hexokinase substrates. (A) Representative mitochondrial ATP responses to glucose withdrawal. **(B)** Representative mitochondrial ATP responses to glucose substitution with 10 mM 2-DG. **(C)** Representative mitochondrial ATP responses to glucose substitution with 10 mM mannose. **(D)** Maximal mitochondrial ATP depletion after glucose removal (white column, N=24/124 cells) or glucose substitution with 2-DG (black column, N=7/31 cells) or mannose (gray column, N=20/80 cells). Mean, SEM, ** $p < 0.01$, *** $p < 0.001$. [Figure panels reproduced from Depaoli et al., Cell Reports 2018.]

3.1.2. Hexokinase 1 and 2 expression levels affect mitochondrial ATP dynamics

Due to the localization of hexokinase 1 and 2 at the outer mitochondrial membrane (OMM) and the interaction with the outer mitochondrial membrane porin VDAC1, it has been speculated that they use mitochondrial ATP to phosphorylate their substrate (9,10,42,81–83). Therefore, and because the transient ATP elevation upon glucose removal was repressed by the addition of other hexokinase substrates such as 2-DG or mannose (**Figure 3.2B-D**), I hypothesized that the peak signal following glucose withdrawal represented the portion of mitochondrial ATP destined for the hexokinase reaction, which would be left over if no substrate was available. Indeed, the simultaneous knock-down of the mitochondria-bound hexokinase isoforms 1 and 2 caused a significant reduction of the peak height, while basal

mitochondrial ATP levels and the maximal depletion of mitochondrial ATP upon glucose removal were not affected (**Figure 3.3A-D**) (42).

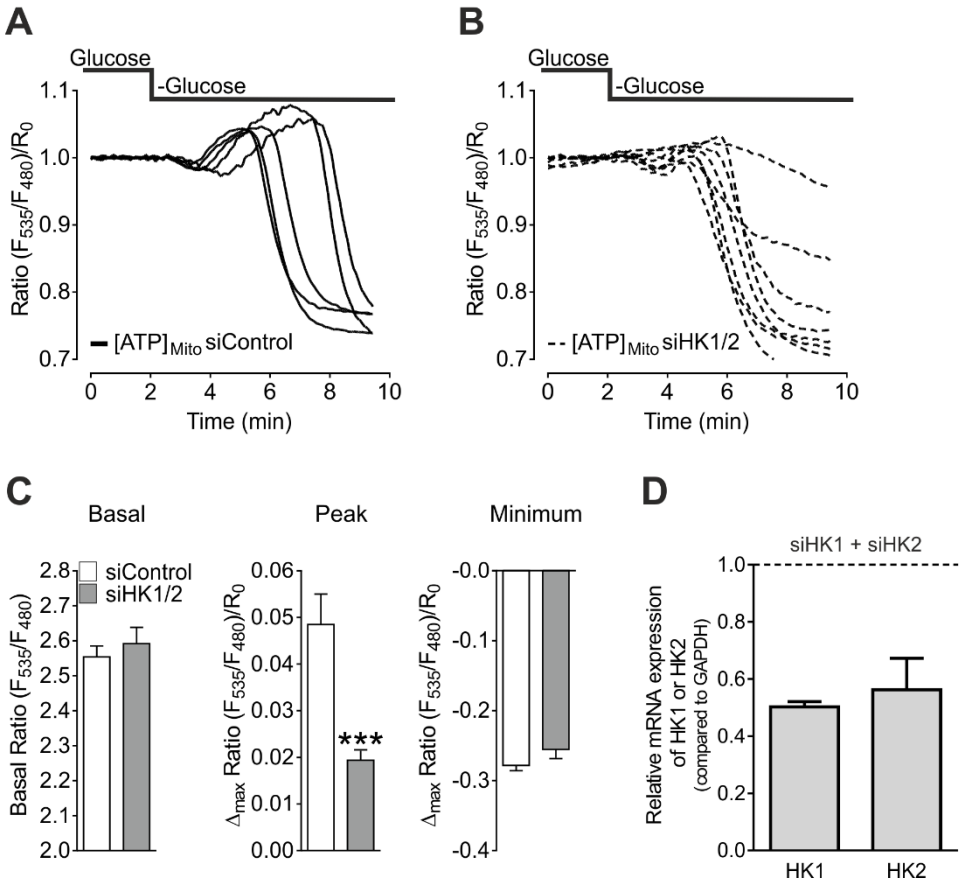

Figure 3.3. Knockdown of hexokinase 1 and 2 affects mitochondrial ATP dynamics. (A) Representative mitochondrial ATP responses to glucose depletion in cells treated with control siRNA (siControl). **(B)** Representative mitochondrial ATP responses to glucose depletion in cells treated with siRNAs against hexokinase 1 and 2 (HK1 and 2). **(C)** Statistical analysis of mitochondrial ATP responses (*left columns*, basal levels; *middle columns*, peak height*; right columns* minimum) to glucose depletion in cells treated with siRNA against hexokinase 1 and 2 (gray columns, N=14/58 cells) compared to cells treated with control siRNA (white columns, N=12/53 cells). Mean, SEM, *** $p < 0.001$ vs siControl. **(D)** Quantification of knock-down efficiency of HK1 or HK2 in HeLa cells after treatment with specific siRNAs via real-time PCR using GAPDH as a reference gene. Mean, SEM, N=3. [Figure panels reproduced from Depaoli et al., Cell Reports 2018.]

Overexpression of GFP-tagged hexokinase 1 or 2 also altered the response of mitochondrial ATP to glucose depletion (**Figure 3.4A-D**). Interestingly, there were more cells without the transient mitochondrial ATP increase in both HK1 (45.5% peak) and HK2 (57.1% peak) overexpressing cells, compared to control cells (100% peak) (**Figure 3.4D**).

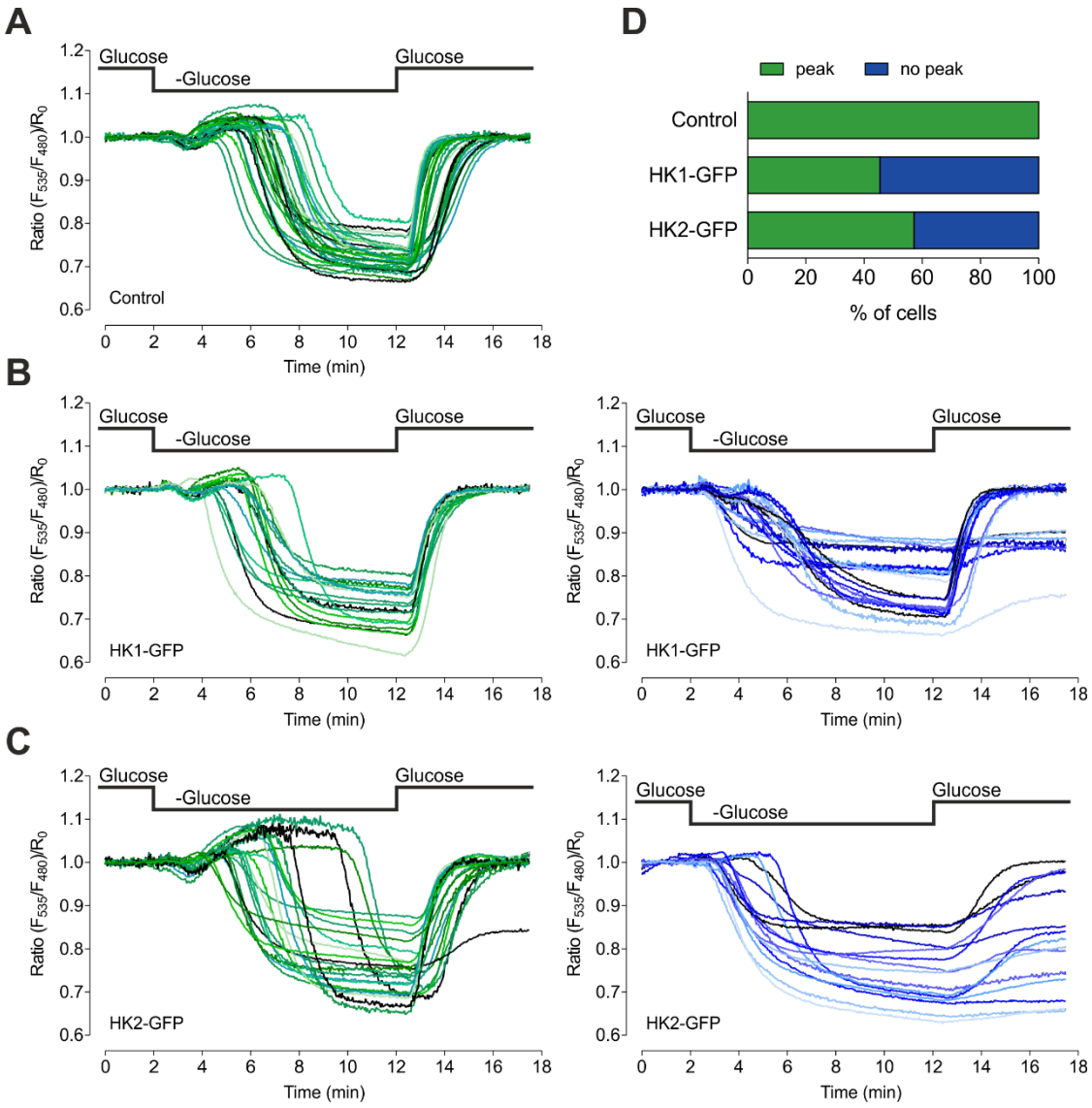

Figure 3.4. Overexpression of HK1-GFP or HK2-GFP affects mitochondrial ATP elevations upon glucose removal. (A) All single cell responses to glucose deprivation of FRET ratio signals of cells expressing mitochondrial ATP probe mtAT1.03 in control cells. **(B)** All single cell responses of mitochondrial ATP to glucose depletion in cells overexpressing HK1-GFP. Cells with transient rise of mitochondrial ATP are presented in the left graph (green), cells without peak in the right graph (blue). **(C)** All single cell responses of mitochondrial ATP to glucose depletion in cells overexpressing HK2-GFP. Cells with transient rise of mitochondrial ATP are presented in the left graph (green), cells without peak in the right graph (blue). **(D)** Percentage of cells with (green) and without peak (blue) in control cells and cells overexpressing HK1-GFP or HK2-GFP, derived from Figure 3.4A-C.

The partial absence of the transient mitochondrial ATP increase upon glucose removal in cells overexpressing hexokinase 1 or 2 was unexpected. A possible explanation would be that under overexpression conditions a certain portion of hexokinases might localize in the cytosol and therefore use cytosolic ATP for glucose phosphorylation. However, high resolution microscopy revealed that HK1-GFP and HK2-GFP both localize to the OMM also under these conditions (**Figure 3.5A-C**) (42). Since hexokinases and VDAC work together on the export of ATP from mitochondria (10,84) and the stoichiometry between these partners is altered if hexokinases are overexpressed, it is likely that the surplus hexokinases bind to the outer mitochondrial membrane, but have no VDAC interaction partner and thus no access to mitochondrial ATP. Hence, overall, cytosolic ATP may be used for the hexokinase reaction instead of mitochondrial ATP.

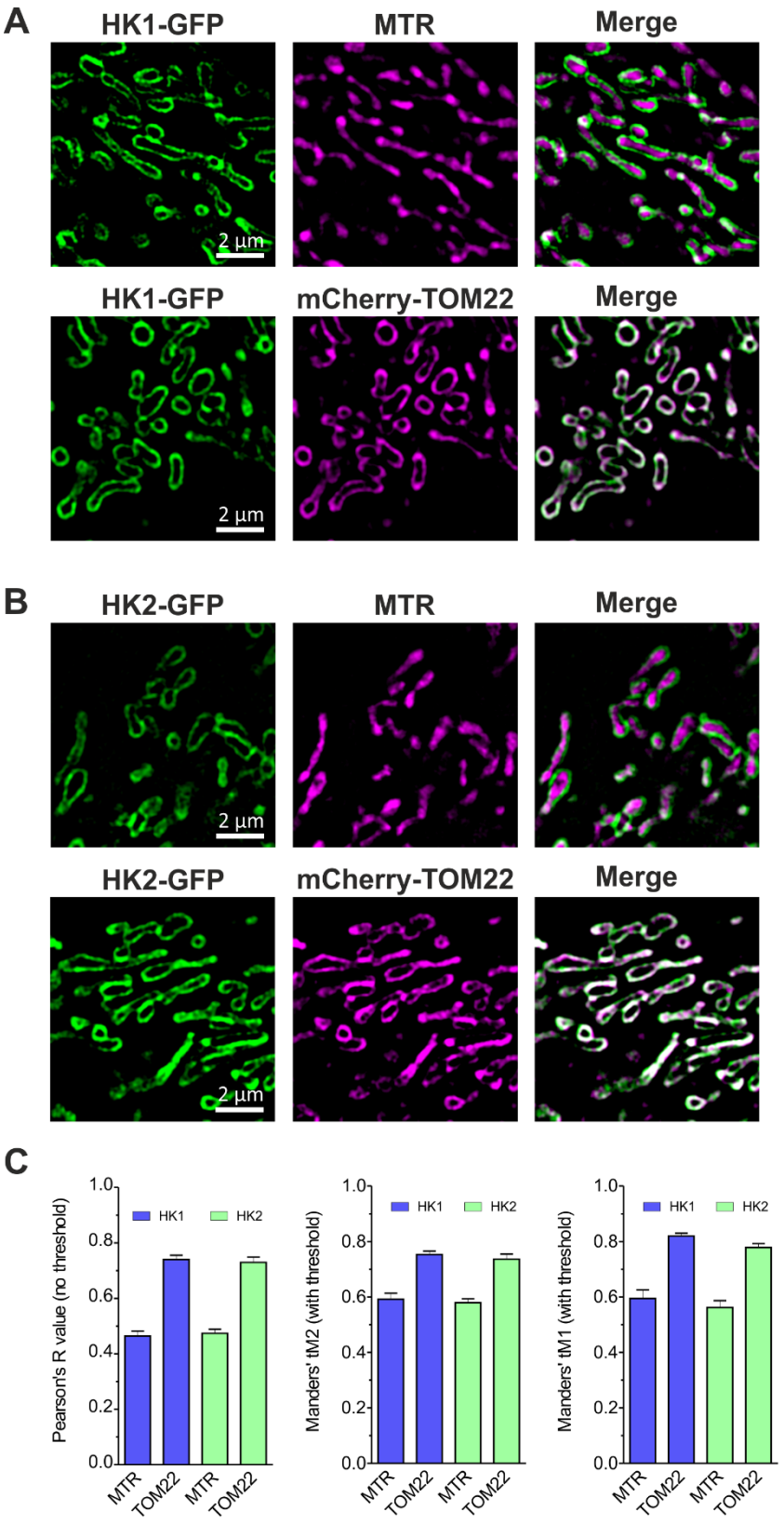

Figure 3.5. Hexokinase (HK) 1 and 2 localization in HeLa cells. (A,B) Representative pictures of hexokinase co-localization experiments with MitoTracker Red FM (MTR) and the OMM marker mCherry-Tom22. **(A)** HK1-GFP and **(B)** HK2-GFP**. (C)** Quantitative analysis of colocalization coefficients Pearson and Manders 1 and 2. Channel 1 represents the GFP and channel 2 the mCherry label. [Figure reproduced from Depaoli et al., Cell Reports 2018.]

3.1.3. Effects of glucose withdrawal on other parameters beyond ATP

To correlate ATP changes with glucose availability, cytosolic glucose levels were measured with the FRET-based glucose sensor FLII^{12}Pglu-700µδ6 (50). Intracellular glucose levels were straightly affected by glucose removal (**Figure 3.6A**) (42). The absence of glycolysis was also reflected in the reduction of the cytosolic NADH/NAD$^+$ ratio, measured with Peredox (57) (**Figure 3.6B**).

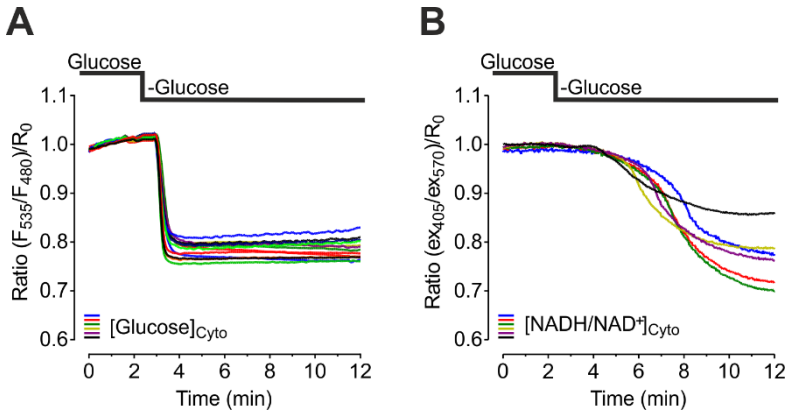

Figure 3.6. Effects of glucose removal on intracellular glucose and NADH levels. (A,B) Representative responses of **(A)** cytosolic glucose levels and **(B)** cytosolic NADH/NAD$^+$ ratios to glucose withdrawal measured with the glucose sensor FLII^{12}Pglu-700µδ6 and the NADH/NAD$^+$ sensor Peredox, respectively. [Figure panels reproduced from Depaoli et al., Cell Reports 2018.]

Next, cytosolic and mitochondrial pH changes in response to glucose removal were measured using genetically encoded ratiometric pH sensors (66), in order to ascertain direct cell physiological consequences of the hexokinase reaction (**Figure 3.7**). Following glucose removal, a transient rise of the cytosolic pH (pH$_{Cyto}$) was observed, followed by a decrease (**Figure 3.7A,C**). Apparently, the alkalization happened at approximately the same time as the rise of mitochondrial ATP, and did not appear in the presence of 2-DG (**Figure 3.7A,C,D**). Since the phosphorylation of glucose (or 2-DG) to glucose 6-phosphate (or 2-DG 6-phosphate) is an acidic reaction, the absence of this reaction likely induces the observed pH$_{Cyto}$ increase. The subsequent pH drop is most probably a consequence of the ATP depletion, e.g. by the hydrolysis of adenine and guanine nucleotides and the inactivation of vesicular H$^+$-ATPase (85). Also the mitochondrial pH dropped during ATP depletion (**Figure 3.7B,C**). In most cells the decline had two phases with different slopes.

The two-step characteristics were also observed in the presence of 2-DG in the case of both mitochondrial and cytosolic pH (**Figure 3.7D,E,F**). The acidification of the cytosol and mitochondria was more pronounced, if glucose was replaced with 2-DG. The acidification was much stronger in mitochondria than in the cytosol in the absence of glucose (**Figure 3.7C**); however, in the presence of 2-DG there was no difference between the two compartments (**Figure 3.7F**).

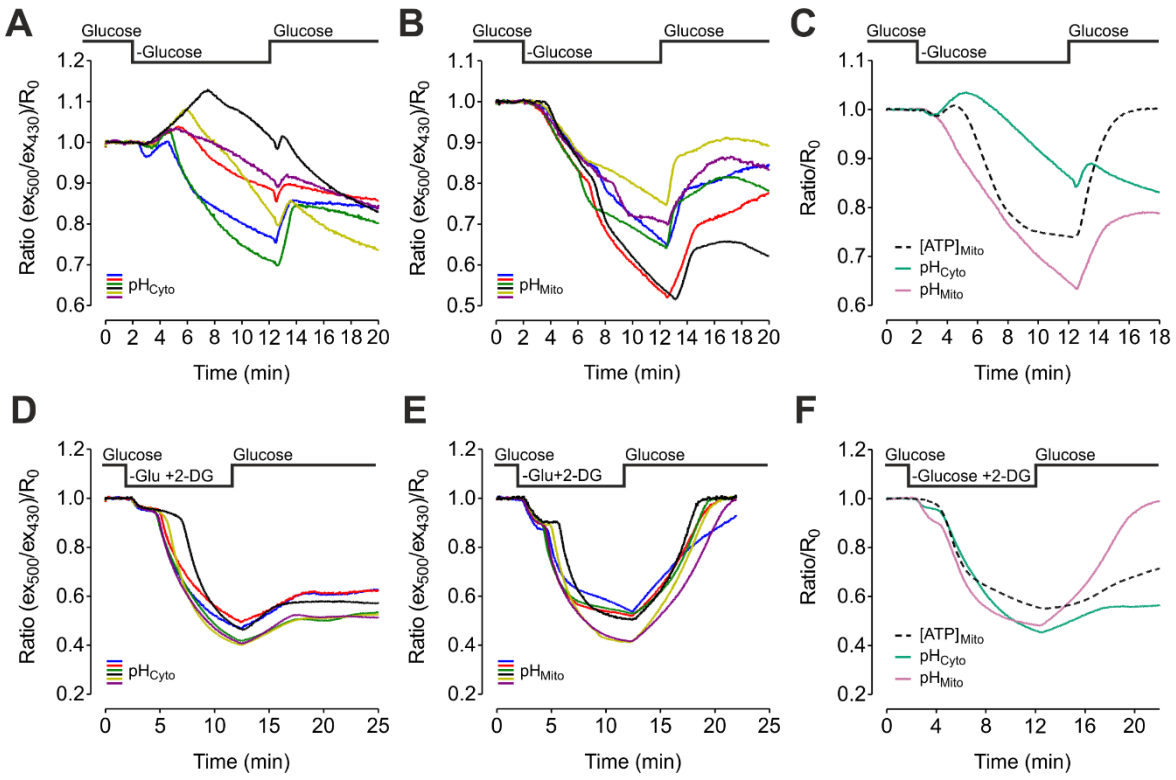

Figure 3.7. Effects of glucose removal on intracellular pH. (A) Representative responses of cytosolic pH to glucose withdrawal, measured with the pH sensor SypHer. **(B)** Representative responses of mitochondrial pH to glucose withdrawal measured with mitochondria-targeted SypHer. **(C)** Mean responses of mitochondrial ATP (N=24/124 cells), cytosolic (N=4/30 cells) and mitochondrial pH (N=4/34 cells) to glucose depletion, calculated from all measurements. **(D)** Representative responses of cytosolic pH to glucose substitution with 2-DG, measured with the pH sensor SypHer. **(E)** Representative responses of mitochondrial pH to glucose substitution with 2-DG, measured with mitochondria-targeted SypHer. **(F)** Mean responses of mitochondrial ATP levels (N=7/31), mitochondrial (N=3/11) and cytosolic pH (N=3/16) to glucose substitution with 2-DG, calculated from all measurements.

3.1.4. Hexokinase reaction may be reversible

After mitochondria-located hexokinases were found to be responsible for the transient ATP increase in the mitochondrial matrix upon glucose removal, I speculated that hexokinases may even be able to produce ATP by converting glucose 6-phosphate to glucose (42). This would also explain the transient increase of mitochondrial ATP upon glucose withdrawal (**Figure 3.1B, Figure 3.2A**); hexokinases may reverse their activity to produce ATP, which would then be transported into the mitochondrial matrix, resulting in a transient ATP increase. To test this hypothesis, a new protocol for mitochondrial ATP measurements was introduced. Cells were first perfused with a glucose free, mannose containing buffer. During that period, mannose was phosphorylated and mannose 6-phosphate accumulated in the cell. After that, also mannose was removed from the cells, causing a strong transient increase of mitochondrial ATP (**Figure 3.8A**) (42). Again, in the absence of any hexose which could be phosphorylated, hexokinases may be able to turn mannose 6-phosphate to mannose and produce ATP causing transient elevations of mitochondrial ATP. This explanation was substantiated by the observation, that silencing of hexokinase 1 and 2 prevented ATP elevations (**Figure 3.8B-D**) (42). The possible reversibility of the hexokinase reaction was also tested with another substrate, namely 2-DG. Cells were perfused with a glucose free buffer containing 2-DG for 10 minutes, to amass 2-DG 6-phosphate within the cells; then 2-DG was also removed from the cells, in order to trigger hexokinases to generate ATP by turning 2-DG 6-phosphtate back to 2-DG (**Figure 3.8E**). The transient mitochondrial ATP elevations were clearly less pronounced than with mannose (**Figure 3.8A,E**), suggesting that the reversibility of the hexokinase reaction was dependent on the substrate. Namely, it appeared that 2-DG 6-phosphate could not be dephosphorylated as efficiently as mannose 6-phosphate, resulting in lower mitochondrial ATP increases (**Figure 3.8A,E**). This would also explain why mitochondrial ATP levels were not completely restored after glucose re-addition if 2-DG was used as substrate (**Figure 3.8E**), because 2-DG 6-phosphate would inhibit hexokinases to some extent and, thus, prevent glucose from entering the glycolytic pathway.

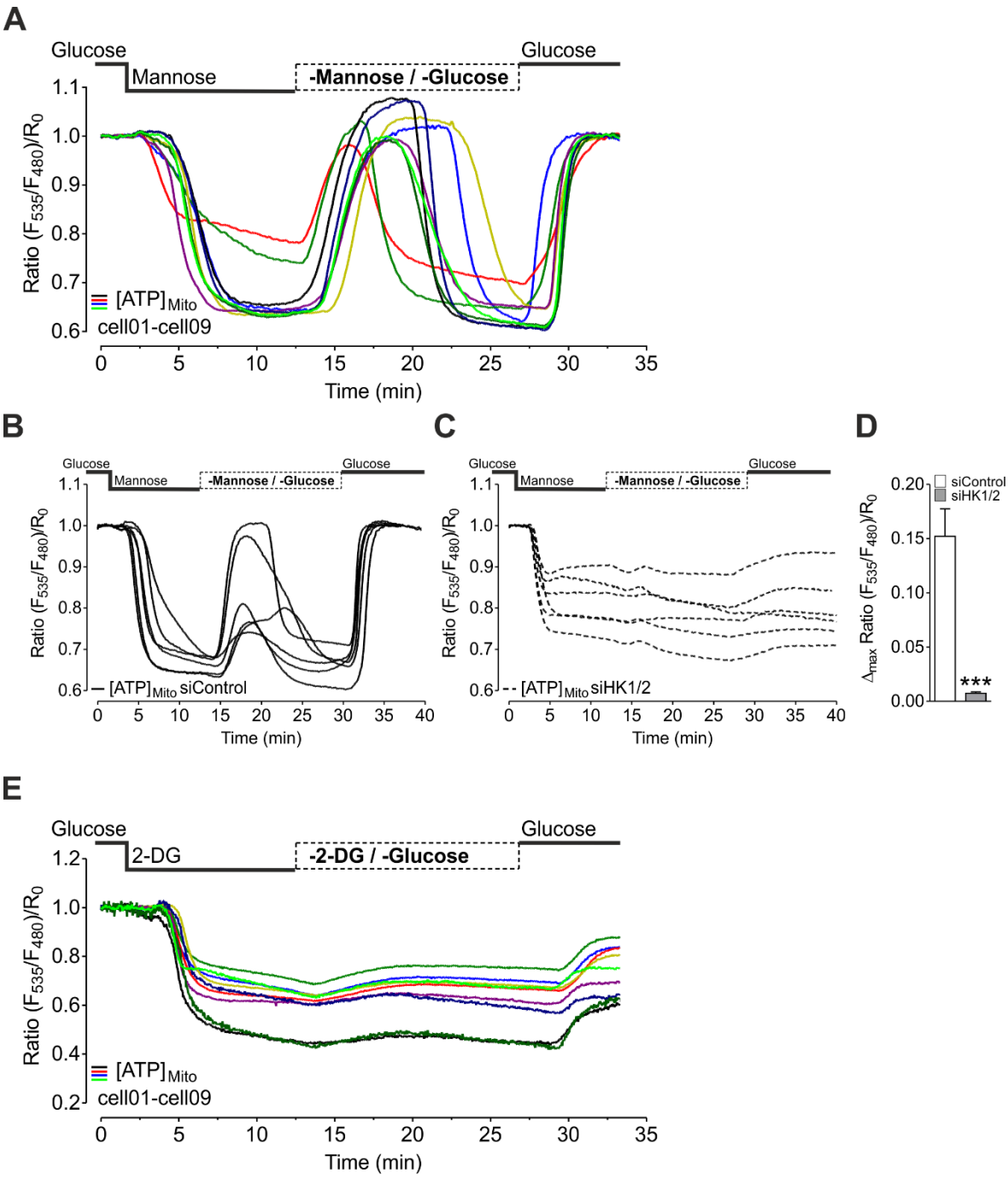

Figure 3.8. Hexokinase reaction may be reversible and fuel mitochondria with ATP. (A) Representative mitochondrial ATP responses to glucose substitution with mannose and subsequent withdrawal of mannose (N=5/25 cells). **(B)** Representative mitochondrial ATP responses to glucose substitution with mannose and subsequent withdrawal of mannose in cells treated with control siRNA (siControl). **(C)** Representative mitochondrial ATP responses to glucose substitution with mannose and subsequent withdrawal of mannose in cells treated with siRNAs against hexokinase 1 and 2 (HK1 and 2). **(D)** Statistical analysis of mitochondrial ATP elevations in response to mannose withdrawal in cells treated with siRNA against hexokinase 1 and 2 (gray columns, N=10/32 cells) compared to cells treated with control siRNA (white columns, N=10/22 cells). Mean, SEM, *** $p < 0.001$ vs siControl. **(E)** Representative mitochondrial ATP responses to glucose substitution with 2-DG and subsequent withdrawal of 2-DG (N=3/13 cells). [Figure panels reproduced from Depaoli et al., Cell Reports 2018.]

3.1.5. Effects of respiratory chain inhibition on mitochondrial ATP in HeLa cells

In order to assess the contribution of mitochondrial respiration to ATP generation, HeLa cells were treated with the respiratory chain inhibitors oligomycin, an ATP synthase F_O portion inhibitor (86), or antimycin A, a complex III inhibitor (87) (**Figure 3.9**). Oligomycin was found to increase mitochondrial ATP levels in most cases, while antimycin A reduced mitochondrial ATP levels. Also the combination of oligomycin and antimycin increased mitochondrial ATP. The difference between oligomycin alone and oligomycin combined with antimycin was not significant, because responses were rather variable.

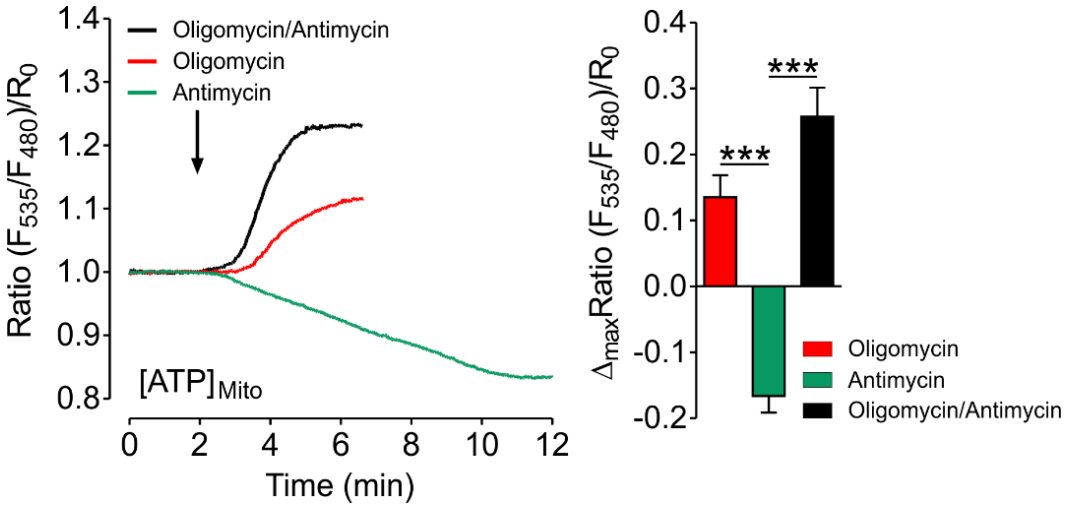

Figure 3.9. Effects of respiratory chain inhibition on mitochondrial ATP. *Left panel*: Normalized responses (mean curves) of mitochondrial ATP levels to treatment with 2 µM oligomycin (red line), 2.5 µM antimycin A (green line), or oligomyin and antimycin A (black line). *Right panel:* Columns represent maximal FRET ratio changes of mtAT1.03 (mean, SEM) upon addition of oligomycin (red column, N=7/49 cells), antimycin A (green column, N=7/22 cells), or oligomycin and antimycin A (black column, N=4/16 cells). *** $p < 0.001$.

These results indicate that (at least under our standard laboratory conditions) in HeLa cells the ATP synthase preferentially runs in its reverse mode, which means, ATP is hydrolyzed to pump protons into the intermembrane space to maintain a hyperpolarized mitochondrial membrane potential (42). As a consequence, the ATP synthase requires more ATP in antimycin A treated cells in order to compensate for the loss of complex III proton pumping activity, causing the expenditure of mitochondrial ATP (**Figure 3.9**).

The next step was to analyze how mitochondrial ATP levels are affected by glucose removal if the ATP synthase is inhibited (**Figure 3.10A**) (42). Oligomycin counteracted mitochondrial ATP depletion and also prevented the transient mitochondrial ATP. Therefore, I tested the possibility that the ATP synthase could be responsible for the transient ATP elevations, with the help of the protocol presented above, where mitochondrial ATP elevations were induced by switching from mannose containing to hexose free buffer (**Figure 3.8**). Here, oligomycin did not prevent mitochondrial ATP elevations (**Figure 3.10B**); the increase was even stronger in the presence of oligomycin (see quantification of the peak width), probably due to the inhibition of ATP hydrolysis by the ATP synthase (42). Thus the ATP synthase is not responsible for the ATP increase upon glucose removal. The absence of the peak upon glucose withdrawal in oligomycin pretreated cells (**Figure 3.10A**) can be explained by the fact, that after the oligomycin induced rise of mitochondrial ATP, no further increase is possible.

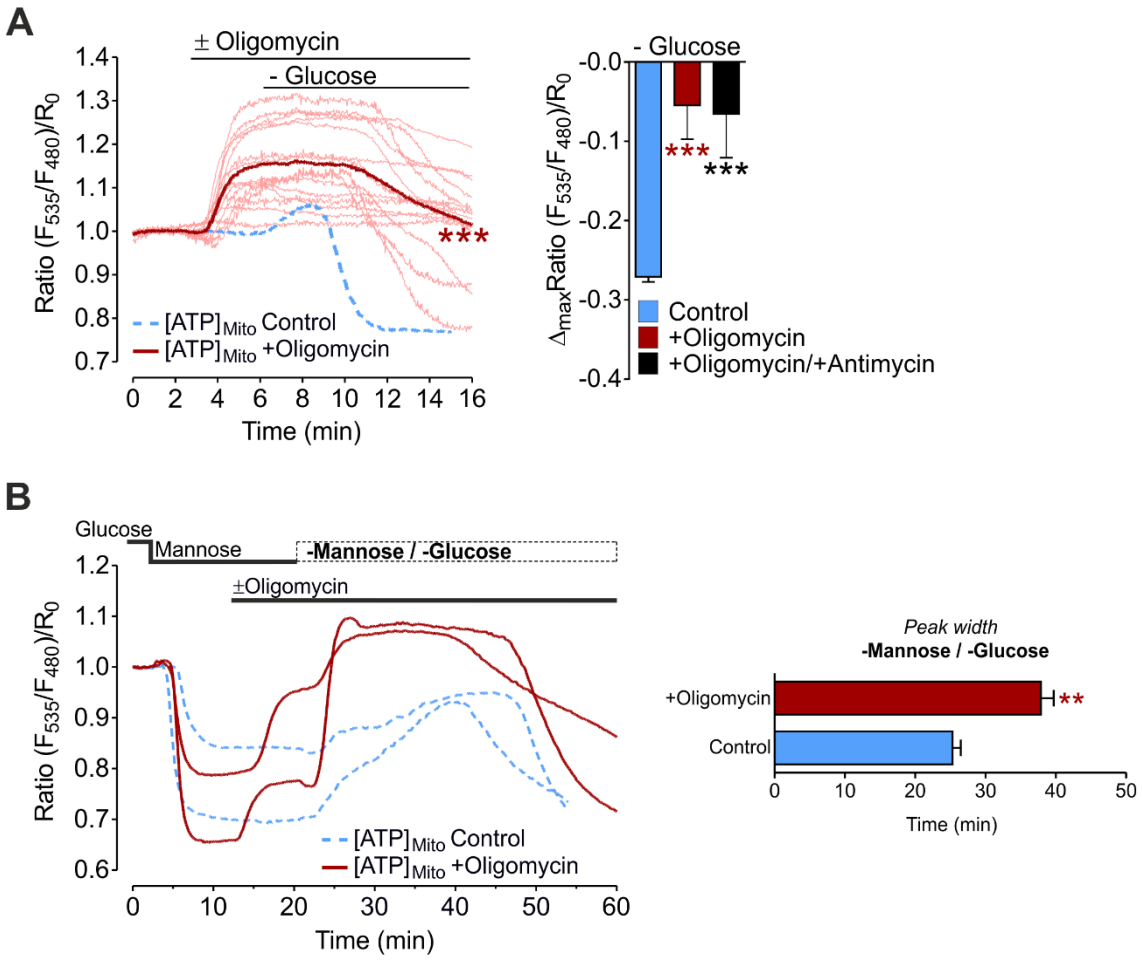

Figure 3.10. ATP synthase does not contribute to mitochondrial ATP elevations upon glucose or mannose removal. (A) *Left panel:* Mitochondrial ATP responses to oligomycin (2 µM) treatment followed by glucose withdrawal in HeLa cells; single cell responses (pale red lines) and mean curve (distinct red line). Blue dashed line shows mitochondrial ATP change upon glucose depletion in the absence of oligomycin. *** $p < 0.001$ vs Control. *Right panel:* Columns represent maximal FRET ratio changes of mtAT1.03 (mean, SEM) upon glucose depletion in the absence (blue column, N=24/111 cells, Control) and presence of oligomycin (2 µM, red column, N=3/15 cells) or oligomycin (2 µM) and antimycin A (2.5 µM) (black column, N=3/8 cells). *** $p < 0.001$. **(B)** *Left panel:* Red solid curves show representative mitochondrial ATP responses to glucose substitution with mannose, followed by oligomycin (2 µM) addition and subsequent withdrawal of mannose in the presence of oligomycin; blue dashed curves show representative mitochondrial ATP responses to the same protocol, but without oligomycin (Control). *Right panel:* Statistical analysis of ATP elevations (peak width) after mannose withdrawal in the presence or absence (Control) of oligomycin. ** $p < 0.01$. [Figure reproduced from Depaoli et al., Cell Reports 2018.]

3.2. Part 2 – Imaging of mitochondrial ATP dynamics for the metabolic profiling of cells

In the first part of this work, I investigated the metabolic activity of HeLa cells. In the second part, I assessed the metabolic setting of different cells types, based on the findings with HeLa cells. For that reason the responses of mitochondrial ATP to glucose depletion and ATP synthase inhibition with oligomycin were measured, in order to determine the contribution of glycolysis and mitochondrial respiration to ATP production (42). The results of the ATP measurements were compared to measurements using respirometry (Seahorse®), where oxygen consumption rate (OCR) was determined as a measure for mitochondrial respiration, and extracellular acidification rate (ECAR) as a measure for the glycolytic activity of a cell. However, even though ECAR is primarily dependent on the glycolytic activity of cells, one needs to consider that the extracellular pH is also affected by the production of succinate and CO_2.

3.2.1. Mitochondrial ATP dynamics in pancreatic β-cells (INS-1, MIN-6)

In contrast to the highly glycolytic HeLa cancer cell line, pancreatic β-cells produce ATP predominantly via mitochondrial respiration. In HeLa cells, mitochondrial ATP declined rapidly and strongly in response to glucose depletion, whereas oligomycin caused an increase of mitochondrial ATP (**Figure 3.11A**) (42). In contrast, glucose removal had only minor effects on mitochondrial ATP levels in both INS-1 (*Rattus norvegicus*) and MIN-6 (*Mus musculus*) β-cells (**Figure 3.11B,C**) (42). The inhibition of the ATP synthase with oligomycin on the other hand was followed by a strong and fast decline of mitochondrial ATP concentrations (**Figure 3.11B,C**). For each cell the maximal ATP change upon glucose depletion was plotted against the maximal change after oligomycin treatment (**Figure 3.11D**). This representation of the results allows the quick classification of cells according to their metabolic activity, as well as the comparison of different cell types or conditions in one graph. For comparison, OCR and ECAR of HeLa and INS-1 cells were measured using respirometry (Seahorse®) and the results were displayed in a similar way by plotting OCR against ECAR (**Figure 3.11E**) (42).

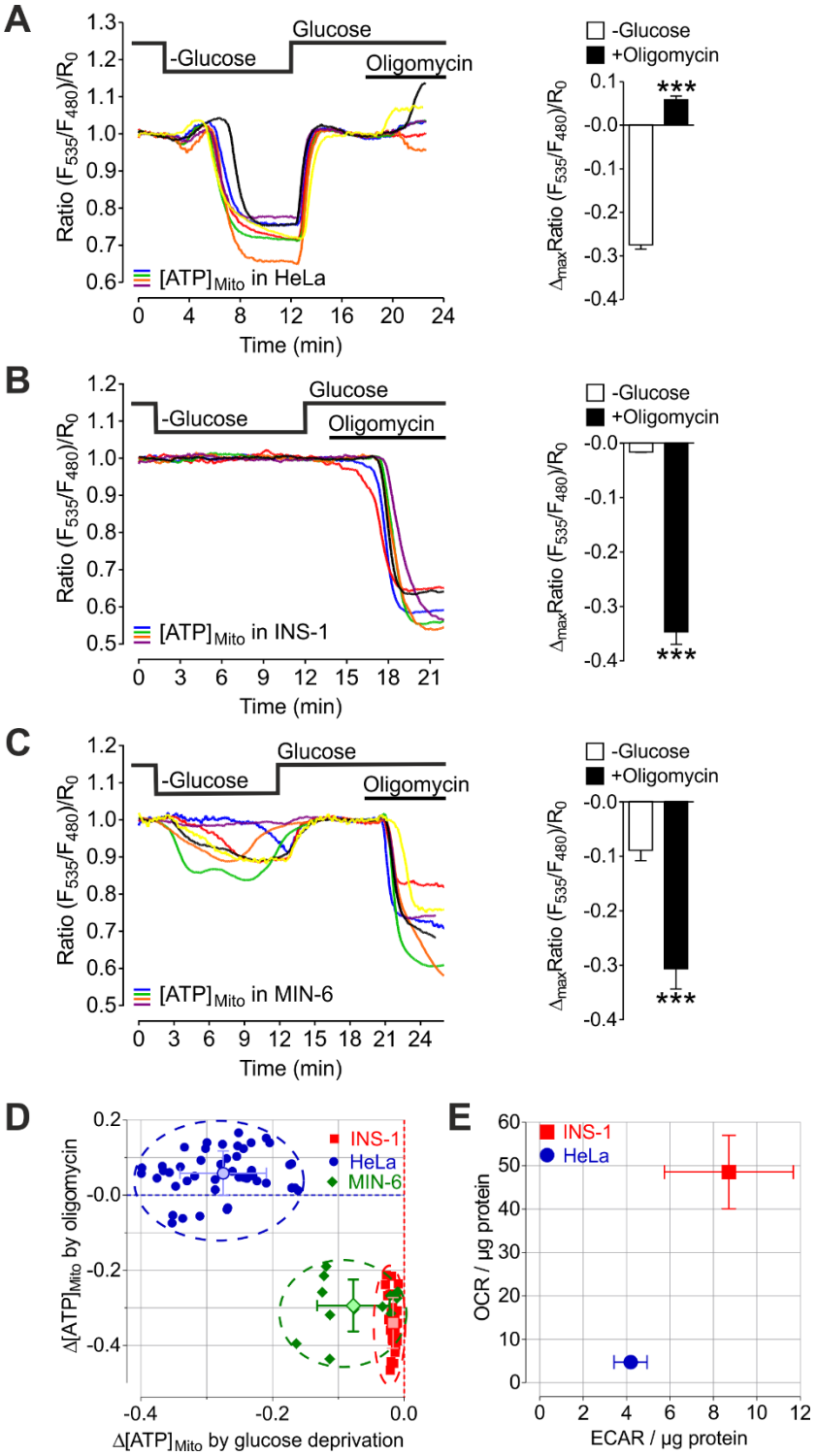

Figure 3.11. Mitochondrial ATP depletion upon glucose deprivation indirectly correlates with mitochondrial respiration. (A-C) *Left panels:* Representative mitochondrial ATP responses of **(A)** HeLa, **(B)** INS-1, and **(C)** MIN-6 cells to glucose depletion and oligomycin (2 µM) treatment. *Right panels:* Statistical analysis of maximal mitochondrial ATP depletion in response to glucose withdrawal and after oligomycin treatment of **(A)** HeLa (N=8/ 47 cells), **(B)** INS-1 (N=4/34 cells), and **(C)** MIN-6 cells (N=4/12 cells). Mean, SEM. *** $p < 0.001$. **(D)** Maximal mitochondrial ATP changes upon oligomycin (2 µM) treatment plotted against maximal mitochondrial ATP changes after glucose removal for HeLa (blue circles, N=8/47 cells), INS-1 (red squares, N=4/34 cells) and MIN-6 cells (green diamonds, N=4/12 cells). In addition, means ± SD are shown. **(E)** OCR plotted against ECAR of HeLa and INS-1 cells measured by respirometry using Seahorse® technology (mean ± SEM, N=3 for both cell types). [Figure panels reproduced from Depaoli et al., Cell Reports 2018.]

3.2.2. Mitofusin 2 ablation and aging affect mitochondrial ATP dynamics in MEFs

In another set of experiments, mitochondrial ATP measurements were used to analyze the effect of mitofusin 2 (Mfn2) knockout and aging on the energy metabolism of mouse embryonic fibroblasts (MEFs) (42). Mfn2 is involved in mitochondrial fusion (88) and the formation of membrane contact sites between mitochondria and the ER (mitochondria associated ER membranes, MAMs) (89). However, it is still a matter of debate, whether Mfn2 supports MAM formation (89) or rather serves as a distance keeper (90). Also reports on the effect of Mfn2 ablation on cell metabolism are controversial. Silencing of Mfn2 impaired mitochondrial respiration (91). Another study, however, showed that the knockout of Mfn2 increased respiratory activity (92). Also in my experiments, Mfn2 knockout markedly affected mitochondrial ATP responses to glucose withdrawal and ATP synthase inhibition in MEFs (**Figure 3.12A-C**) (42). While wild-type MEFs (low passages, below 50) depended on glycolysis for ATP production (**Figure 3.12A,C**), Mfn2 knockout cells produced ATP preferably via mitochondrial respiration (**Figure 3.12B,C**). Intriguingly, at higher passage numbers (above 90) also wild-type MEFs shifted from glycolysis to oxidative phosphorylation (**Figure 3.12D,F**), while Mfn2 knockout had no further effect (**Figure 2.12E,F**) (42). Interestingly, measurements of oxygen consumption rate (OCR) and extracellular acidification rate (ECAR) using respirometry (e.g. Seahorse®) showed fewer differences between young wild-type MEFs and young Mfn2 knockout MEFs (**Figure 3.12G**) compared to the single cell mitochondrial ATP imaging approach (**Figure 3.12A-F**) (42).

It is difficult to figure out, why it was not possible to resolve the differences between wild-type and Mfn2 knockout cells by measuring OCR and ECAR. As previously mentioned, ECAR might also be influenced by other processes apart from glycolysis. Furthermore, cells had to be 100% confluent for Seahorse® measurements, while ATP measurements were performed at a confluency of 80 to 90%, which might have impacted their metabolic activity. Anyhow, in order to ascertain the contribution of different energy-producing pathways, measuring mitochondrial ATP is certainly the more direct method.

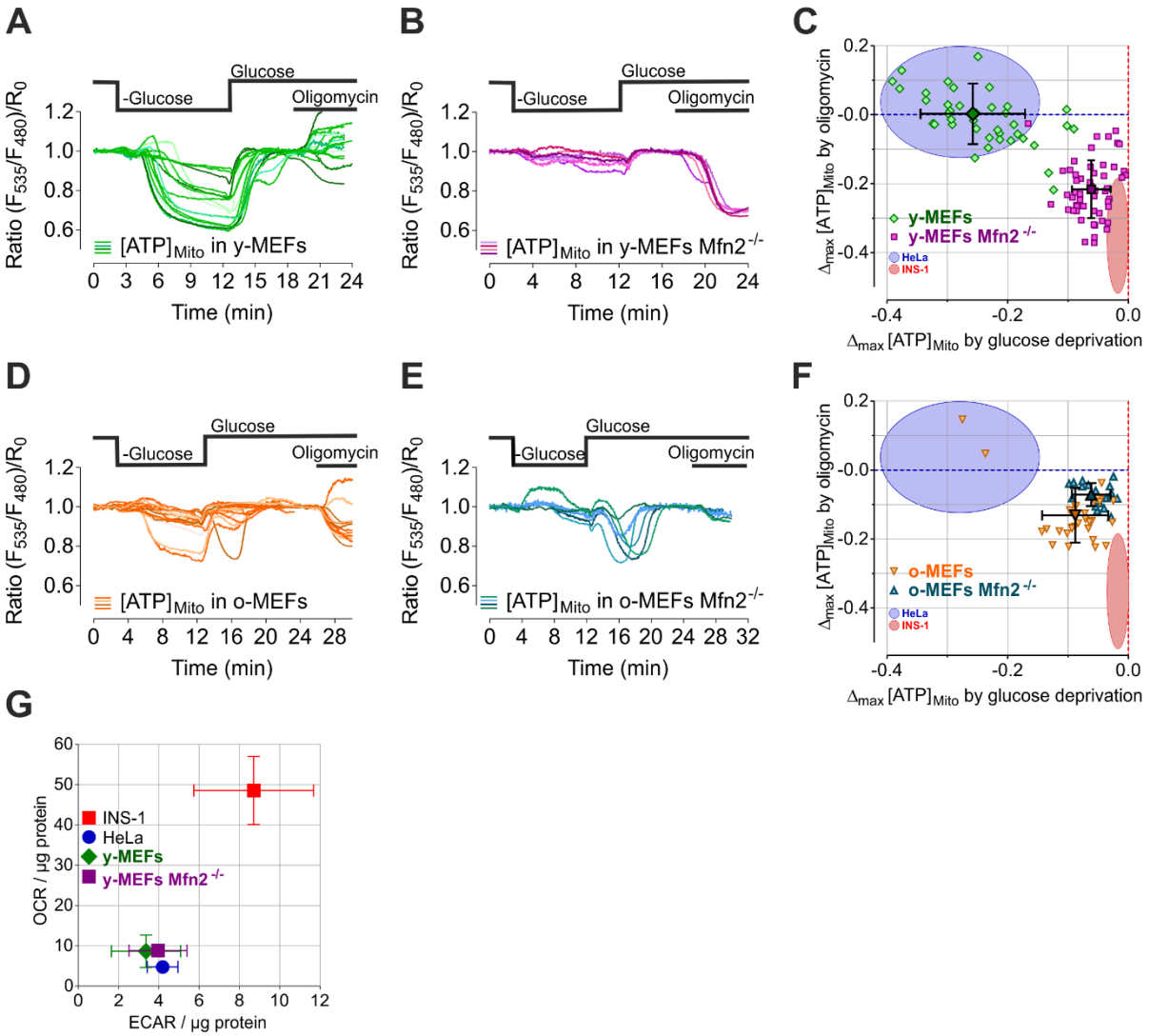

Figure 3.12. Cellular aging and ablation of Mfn2 specifically alter mitochondrial ATP dynamics in MEFs. Representative mitochondrial ATP responses to glucose depletion and inhibition of the ATP synthase with oligomycin (2 µM) in **(A)** young/low passages wild-type MEFs (y-MEFs), **(B)** young Mfn2$^{-/-}$ MEFs, **(D)** old/high passages wild-type MEFs (o-MEFs), and **(E)** old Mfn2$^{-/-}$ MEFs. **(C,F)** Single cell maximal mitochondrial ATP depletion induced by oligomycin plotted against maximal ATP depletion upon glucose depletion (mean, SD). **(C)** Comparison of young/low passages wild-type MEFs with young/low passages Mfn2$^{-/-}$ MEFs. **(F)** Comparison of old/high passages wild-type MEFs with old/high passages Mfn2$^{-/-}$ MEFs. **(G)** Oxygen consumption rates (OCR) plotted against extracellular acidification rates (ECAR) of young wild-type MEFs (y-MEFs) and young Mfn2$^{-/-}$ MEFs compared to HeLa and INS-1 cells, determined by respirometry using Seahorse® technology. Mean, SEM, N=3. [Figure reproduced from Depaoli et al., Cell Reports 2018.]

3.2.3. Mitochondrial ATP dynamics in cancer cell lines

It is well known, that the metabolism of cancer cells differs considerably from their non-transformed counterparts. In addition, analyses of cancer cell bioenergetics have revealed, that there are also great differences between various cancer cell types, and also among

different cells of one cell type. And even here sub-populations exist, which often make it difficult to eliminate all cancer cells and prevent recurrence. As shown with HeLa and other, non-cancer cells, mitochondrial ATP dynamics are cell-type specific. Therefore, it was standing to reason to use mitochondrial ATP measurements for the metabolic profiling of cancer cells. To test the applicability of this approach for the characterization of cancer cells, I chose three well known breast cancer cell lines (MCF-7, MDA-MB231, SkBr3), as well as three widely used lung adenocarcinoma cell lines (H1299, A549, Calu-3) and the neuroblastoma cell line SH-SY5Y.

First, respirometry was used to measure OCR and ECAR (**Figure 3.13A**). All cancer cell lines showed similar results with a low OCR, indicative of a low respiratory activity (42). On the other hand, mitochondrial ATP measurement revealed great differences between the cancer cell lines (**Figure 3.13B-H, Figure 3.14A-G**), while basal glucose levels and glucose turnover were very similar (**Figure 3.14 H,I**) (42). In addition, the responses among individual cells of one cell line were rather heterogeneous (**Figure 3.13B-H, Figure 3.14A-G**). Interestingly, MDA-MB231 breast cancer cells were most similar to HeLa cells with respect to mitochondrial ATP dynamics (**Figure 3.13G, Figure 3.14F**). All other tested cancer cell lines tended to produce less ATP via aerobic glycolysis and were more dependent on oxidative phosphorylation (**Figure 3.13B-H**).

Also the initial responses of mitochondrial ATP to glucose removal varied widely among the different cancer cell lines (**Figure 3.14A-G**). Already with HeLa cells (**Figure 3.2A**), but in particular in view of the other cancer cell lines, one could make out three phases during the response to glucose withdrawal. First there is a drop of mitochondrial ATP (often not observed), then an increase (not always observed), and finally the decline to minimal ATP levels. Most likely, two processes are responsible for the appearance of the curve. One is the depletion of mitochondrial ATP resulting from the lack of ATP supply from glycolysis. The second process is the increase of mitochondrial ATP, possibly by a hexokinase mediated mechanism (*see Part 1, Chapter 3.1*). The specific run of the curve most likely depends on when and how strong the increase appears. In this aspect, there is a large heterogeneity among different cell lines and also among individual cells of the same cell line (**Figure 3.13B-H, Figure 3.14A-G**).

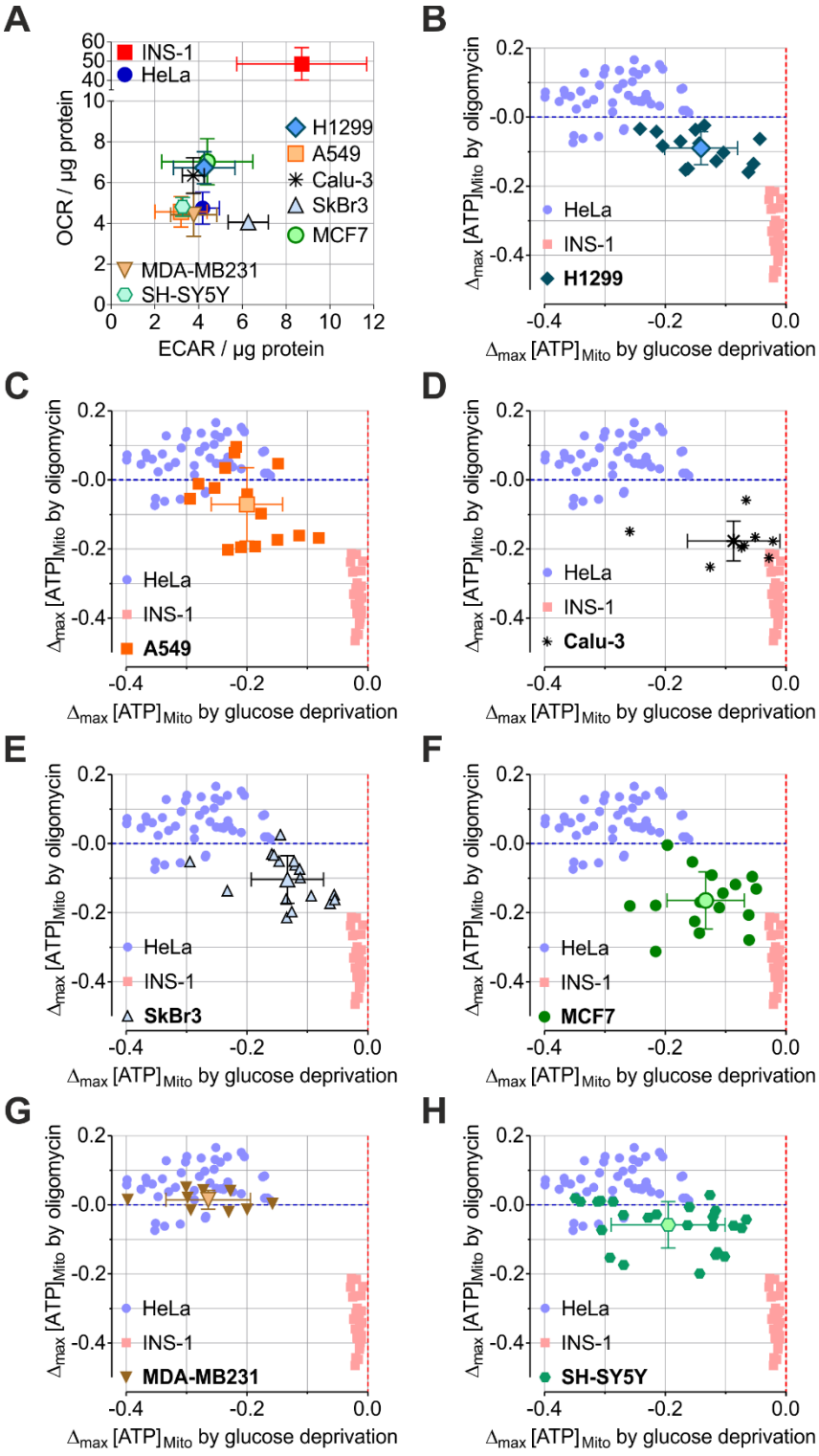

Figure 3.13. Imaging of mitochondrial ATP dynamics in single cancer cells reveals distinct metabolic settings. (A) Oxygen consumption rate (OCR) and extracellular acidification rate (ECAR) of different cancer cell lines (H1299, A549, Calu-3, SkBr3, MCF7, MDA-MB231, SH-SY5Y) and HeLa and INS-1 cells for comparison. Mean, SEM, N=3. **(B-H)** Single cell maximal mitochondrial ATP changes induced by oligomycin (2 µM) plotted against maximal ATP changes upon glucose depletion for **(B)** H1299, **(C)** A549, **(D)** Calu-3, **(E)** SkBr3, **(F)** MCF7, **(G)** MDA-MB231, and **(H)** SH-SY5Y cells, as well as HeLa and INS-1 cells for comparison; in addition means ± SD are shown. [Figure reproduced from Depaoli et al., Cell Reports 2018.]

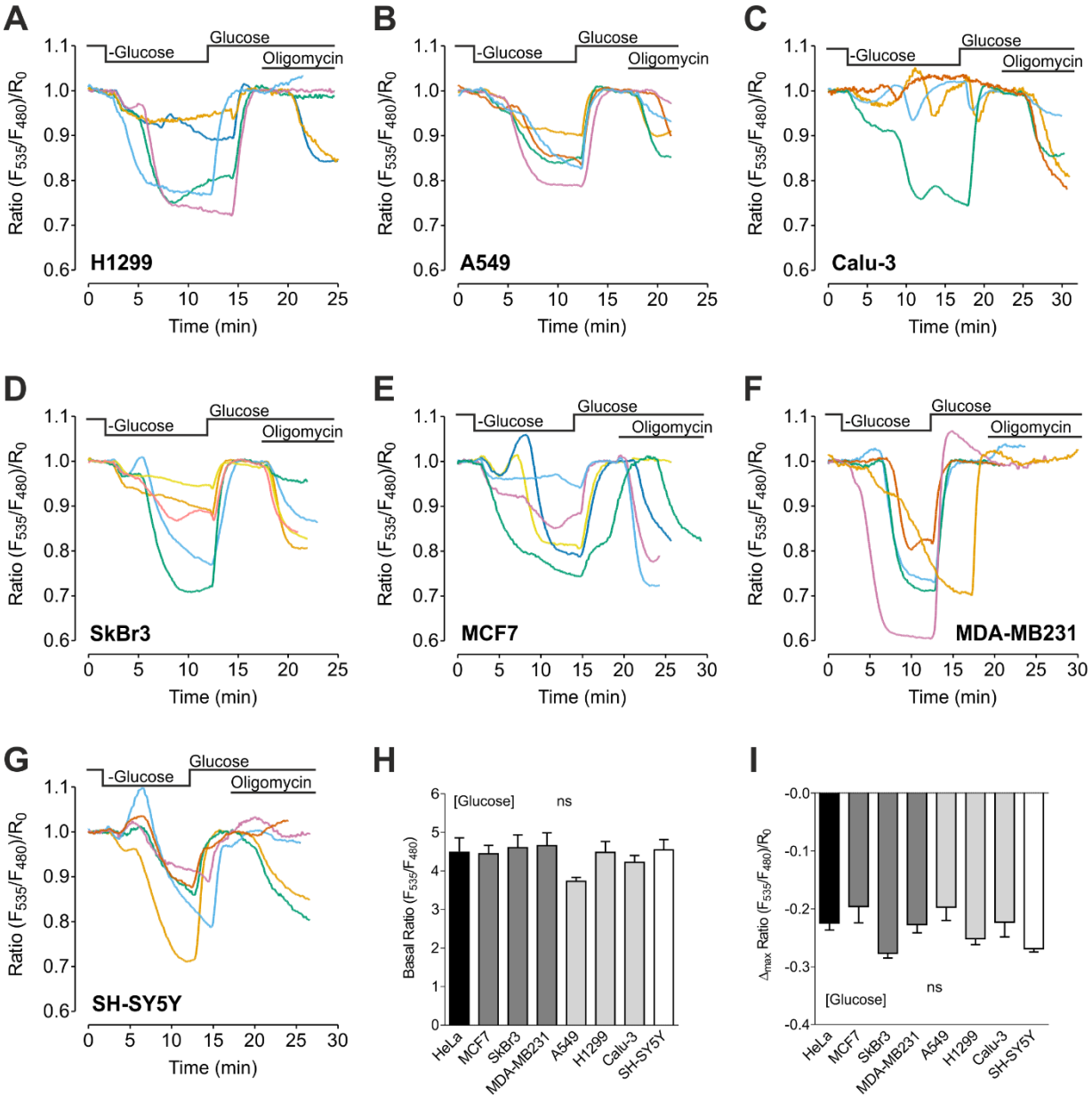

Figure 3.14. Single cell responses of mitochondrial ATP levels to glucose deprivation in different cancer cell lines. (A-G) Representative mitochondrial ATP curves of **(A)** H1299, **(B)** A549, **(C)** Calu-3, **(D)** SkBr3, **(E)** MCF7, **(F)** MDA-MB231, **(G)** SH-SY5Y cancer cells. **(H)** FRET ratio signals (mean, SEM) of cytosolic glucose sensor in different cancer cell lines in the presence of 10 mM glucose in the extracellular medium. **(I)** Maximal FRET changes of the cytosolic glucose sensor upon complete removal of glucose. ns not significant. [Figure panels reproduced from Depaoli et al., Cell Reports 2018.]

4. Discussion

In this work, I primarily investigated the response of subcellular ATP levels to glucose starvation and, based on that, established a protocol for the metabolic profiling of cells using mitochondrial ATP measurements.

4.1. Mitochondrial ATP levels are highly dynamic, also in glycolytic cancer cells

Cancer is associated with profound metabolic changes (19,93), which have been investigated intensely over the past decades. In order to expand our understanding of this fundamental aspect of cancer, I used genetically encoded fluorescent ATP sensors to measure intracellular ATP levels in HeLa cells, as a cancer model. Like most cancer cells, HeLa cells produce ATP via high rates of glycolysis. Although glycolysis takes place in the cytosol, I observed that glucose withdrawal mainly affects mitochondrial ATP levels. Cytosolic ATP levels, however, are more constant, probably due to the activity of energy stress sensors, such as AMP-activated protein kinase (AMPK) (42,94). Low ATP/ADP or ATP/AMP ratios activate AMPK, which turns off energy consuming processes while ATP producing processes are up-regulated (95). The fast and strong dynamic changes of mitochondrial ATP upon glucose removal and re-addition suggest that glycolytic ATP is delivered into mitochondria in large quantities, and consumed by reverse ATP synthase activity. This rather unexpected finding implies that mitochondria also essentially contribute to ATP production in this cells type, albeit not by synthesis of ATP via respiratory chain activity, but indirectly by controlling ATP fluxes and turnover. Specifically, the steady transport of ATP into mitochondria might be an important driving force for the high glycolytic activity of cancer cells, as it counteracts the repression of glycolysis by high ATP/ADP+AMP ratios (42). In addition, ATP apparently fulfills a function within HeLa cell mitochondria as well, by fueling the reverse activity of the ATP synthase. The ATP synthase hydrolyzes ATP to pump protons across the inner mitochondrial membrane, in order to maintain a negative mitochondrial membrane potential, which is essential for cell survival, e.g. by maintaining mitochondrial protein import and mitochondrial Ca^{2+} homeostasis, and preventing apoptotic cell death. As

respiration is low in most cancer cells, proton extrusion must be achieved by other means, such as the reverse activity of the ATP synthase. Importantly, mitochondria certainly contribute to cellular energy homeostasis, also in cancer cells. The direction of ATP transfer between the cytosol and mitochondria might be integral for cancer cell metabolism, and ATP transporters may be key players in establishing cancer-associated metabolic alterations (42). High levels of ANT2 expression for example are connected with a glycolytic metabolism and cancerogenesis (96). Hence, future studies should focus on studying the role of mitochondrial ATP transporters, such as different ANT isoforms, in cancer cell metabolism, possibly also by using live-cell imaging of subcellular ATP dynamics.

4.2. Hexokinase links glycolysis to mitochondrial ATP

The first step of the glycolytic pathway is the phosphorylation of glucose to glucose 6-phosphate. This step is catalyzed by hexokinase and requires the investment of ATP. There are four different hexokinase isoforms, hexokinase 1, 2, 3 and 4; hexokinase 4 is better known as glucokinase (9). The 100 kDa proteins hexokinase 1, 2 and 3 are thought to have originated from a 50 kDa ancestral form. Hexokinase 1 is found in all mammalian tissues, and is considered a housekeeping enzyme, which is unaffected by most physiological, hormonal, and metabolic changes. Hexokinase 2, on the other hand, is subject to regulation in many cell types, for instance via the AKT/mTOR pathway (83), and expression levels of this isoform are increased in many cancers (9). Hexokinase 3 is substrate-inhibited by physiological glucose concentrations, but little is known about the regulatory characteristics of this isoform (9). However, hexokinase 3 has been identified as a key factor in pediatric acute lymphoblastic leukemia (ALL) (97). All isoenzymes share high sequence similarities. As mentioned before, both hexokinase 1 and 2 associate with the outer mitochondrial membrane. As previously described (9,98,99), the existence of more than one isoform may play an important role in cell physiology. The different isoforms may help to distribute glucose 6-phosphate among different pathways (glycolysis, glycogen synthesis, pentose phosphate pathway). Therefore, I think that changes in the expression levels or regulation of the hexokinase isoforms could drastically affect cell metabolism, which could even contribute to the development of cancer or other diseases.

The characteristic response of mitochondrial ATP levels to glucose depletion revealed that mitochondria-associated hexokinases link glycolytic ATP production with the mitochondrial ATP pool (42). Due to the localization at the outer mitochondrial membrane and the interaction with the VDAC1 it has been proposed that hexokinase 1 and 2 are fueled by mitochondrial ATP (9,10,81–83). However, without solid evidence this idea has remained hypothetical. The results presented in this work now strongly indicate that the activity of hexokinase 1 and 2 is indeed coupled to the mitochondrial ATP pool (42). In addition, mitochondrial ATP measurements revealed that the hexokinase reaction might be reversible (42). That means, glucose 6-phosphate could possibly be turned to glucose, thereby producing ATP, which is transferred into the mitochondrial matrix. This has been proposed before (96), although the hexokinase reaction is widely considered irreversible (100). However, the assumption that the hexokinase reaction was irreversible is based on in vitro studies with purified enzymes, which might only poorly reflect the reaction conditions in living cells. In particular, the association with mitochondria and the coupling to the mitochondrial ATP pool might allow the reversal of the hexokinase reaction (42). The reversal of the hexokinase activity is not the only possible explanation for the transient elevations. Alternatively, the peak could result from the release of ATP bound to mitochondria-associated hexokinases, induced by the absence of any substrate (e.g. glucose, mannose, 2-DG) (42). The peak height would depend on the activity of mitochondrial hexokinase enzymes and mitochondrial ATP concentrations. Low mitochondrial ATP concentrations as well as the depolarization of the mitochondrial membrane potential favor ATP import (101). However, the implications of the hexokinase association with mitochondria and the mitochondrial ATP pool remain to be investigated in more detail in further studies. One promising approach is to induce the detachment of hexokinase 2 from mitochondria using a cell-permeable peptide analog of the hexokinase 2 VDAC binding domain (102).

A similar peptide with a different internalization sequence was successfully used is a study on the role of hexokinase 2 in apoptosis (103). This work showed that hexokinase dissociation from mitochondria induced cell death independent of VDAC, opposing the prevailing view at that time, that hexokinase detachment triggered apoptosis via VDAC

dependent permeabilization of the outer mitochondrial membrane. The protective effects of mitochondria-associated hexokinase 2 are currently explained by antagonizing the binding of apoptotic Bcl-2 family proteins to mitochondria (83,102,104–107). The anti-apoptotic functions of hexokinase are also are considered as one of the reasons for the enhanced hexokinase expression in many cancer cells. In addition, mitochondria-associated hexokinase 2 has also been shown to reduce ROS formation and counteract the opening of the mitochondrial permeability transitions pore (mPTP) (80,108–111). In view of the involvement of hexokinases in apoptosis, and also in preventing ROS formation and mPTP opening (83), one can speculate about the relationship between these processes and the metabolic functions of hexokinases, as they were investigated in this thesis. Future studies should therefore aim to provide more clarity in this context, in addition to data emphasizing the role of Akt kinase in mediating metabolic and pro-survival functions of hexokinase 2 (83).

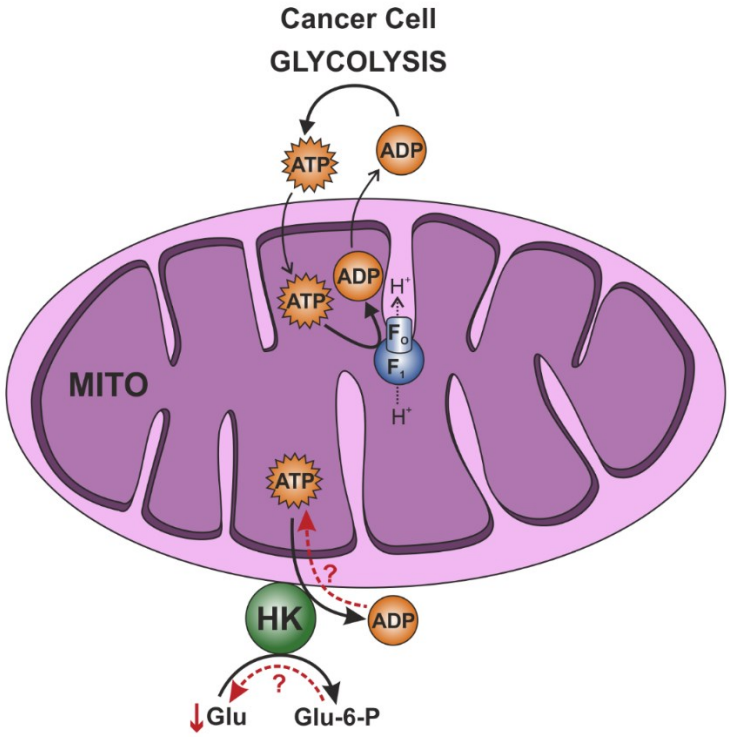

Figure 4.1. Hexokinase links glycolysis to mitochondrial ATP. This model shows how cancer cell glycolysis may be linked to mitochondria, based on the results presented in this work. Mitochondria-located hexokinases use mitochondrial ATP to phosphorylate glucose in the first step of glycolysis. This reaction seems to be reversible in the absence of glucose. On the other side, ATP generated via glycolysis is transported into mitochondria, where it is consumed by the ATP synthase running in reverse mode. That means the ATP synthase hydrolyzes ATP to pump protons across the inner mitochondrial membrane, in order to maintain a hyperpolarized membrane potential. [Figure reproduced from Depaoli et al., Cell Reports 2018.]

4.3. Compartmentalization of glycolysis – a short digression

In view of the fact, that hexokinases are closely linked to mitochondria, I believe that the localization of glycolytic enzymes might be important for the regulation of glycolysis. Therefore, I will give a short review on literature concerning glycolytic compartments.

Recently, it has been shown that in the single-celled parasitic stramenopile *Blastocystis* three glycolytic enzymes of the "pay-off phase" of glycolysis have a mitochondrial targeting sequence and localize within mitochondria (112) The same study describes the existence of similar mitochondrial targeting sequences in enzymes of other stramenopiles. Although these mitochondrial targeting sequences seem to be specific for stramenopiles, this is still a remarkable example of how compartmentalization of glycolytic activities might be advantageous for an organism. Similar to cancer cells, the anaerobe organism *Blastocystis* relies on glycolysis for ATP production (112). The separation of the investment and pay-off phase of glycolysis may help to prevent that those steps are mixed up (112). In cancer cells a similar effect might be achieved by shuttling ATP, which is predominantly produced in the cytosol by aerobic glycolysis, into mitochondria, a view supported by the data presented in this thesis.

Trypanosoma brucei and other protozoa of the *Kinetoplastida* even have a glycolytic organelle – the glycosome – which belongs to the peroxisome family of organelles (113,114). Depending on the environment, these parasites switch between different ATP producing pathways (aerobic and anaerobic glycolysis, as well as mitochondrial respiration). The compartmentalization of glycolytic enzymes in glycosomes allows fast metabolic adaptations by the controlled setup and dismantling of whole glycosomes (114). In *T. brucei*, the first seven enzymes of glycolysis are located in the glycosome, while the last steps of glycolysis take place in the cytosol (113). Thus, the net production of ATP is achieved in the cytosol. As in the case of stramenopiles, the separation of ATP consuming and ATP producing events may prevent that those steps are confused and thereby help to maintain high rates of glycolysis. A similar dynamic reorganization of glycolytic complexes might contribute to the metabolic flexibility of mammalian cells.

Other studies also point at the existence of glycolytic compartments as a temporary phenomenon in physiological contexts. A study by Jang et al. from 2016 (115), for instance, identified a so called "glycolytic metabolon" in *Caenorhabditis elegans* neurons, a term describing the assembly of glycolytic enzymes at presynaptic sites under conditions of energy stress. This "glycolytic metabolon" is considered to serve local ATP production at the sites where it is needed. Similar to the transport of mitochondria to synapses (116–118), glycolytic enzymes (phosphofructokinase 1.1, glyceraldehyde-3-phosphate dehydrogenase 3, fructose-bisphosphate aldolase 1) were also shown to localize to presynaptic sites to build a "glycolytic metabolon" under hypoxic conditions as well as under normoxic conditions during high neuronal activity or in case of mitochondrial dysfunction (115). In addition, this study likewise demonstrated how subcellular ATP imaging could be used to study cell physiology.

As already indicated before, the association of glycolytic enzymes with mitochondria would make sense for the coordination between glycolysis and oxidative phosphorylation. In a proteomic screen, Giegé et al. found seven of the glycolytic enzymes in the mitochondrial fraction of *Arabidopsis thaliana* cells, namely hexokinase, fructose-bisphosphate aldolase, triosephophate isomerase, glycerinaldehyde-3-phosphate dehydrogenase, phosphoglycerate mutase, enolase and pyruvate kinase (119). Although the three remaining enzymes (phosphoglucose isomerase, phosphofructokinase, and phosphoglycerate kinase) were not found, their activity could be measured in isolated *A. thaliana* mitochondria. However, only pyruvate kinase had a mitochondrial targeting sequence. The same study showed that YFP labeled aldolase and enolase localize in the cytosol, but concentrate at mitochondria (119). Since the activity of all glycolytic enzymes was abolished after protease treatment of the isolated mitochondria, they are most likely located at the OMM, where they are not protected. In summary, approximately 5 to 10% of the cytosolic isoforms of all glycolytic enzymes were bound to mitochondria.

In a follow up study the same group describes, how cells may benefit from the dual localization of glycolytic enzymes (120). They found that the degree of mitochondrial association of glycolytic enzymes was dependent on the respiratory rate in both *Arabidopsis* cells and potato (*Solanum tuberosum*) tubers, and that the mitochondrial association is

important for substrate channeling. Upon inhibition of respiration with KCN, the association of glycolytic enzymes with mitochondria decreased. The total glycolytic activity, however, stayed the same. Therefore, they concluded that there was a repartition of the glycolytic activity to the cytosol, if mitochondrial respiration was impaired. The authors explain two reasons for the mitochondrial localization of glycolytic enzymes; first, to efficiently provide pyruvate to mitochondrial respiration; second, the association with mitochondria may help to build glycolytic complexes, which would allow efficient glycolysis via substrate channeling.

In the context of these considerations on glycolytic compartmentalization, the results presented in this study – in particular with regard to subcellular ATP dynamics and the role of the hexokinase enzyme – could serve as a starting point for a more detailed investigation of how energy metabolism is organized on subcellular level. In particular, it would be worthwhile to investigate whether glycolytic compartments exist and how cancer cells may benefit from their reorganization. It is tempting to speculate, that the formation of certain metabolic complexes might even contribute to the development of cancer.

4.4. Metabolic profiling with the help of mitochondrial ATP measurements

The second part of this thesis demonstrates that mitochondrial ATP measurements allow the metabolic profiling of individual cells. Depending on the metabolic setting of a cell, mitochondrial ATP was found to respond differently to glucose removal and inhibition of mitochondrial ATP production by oligomycin (42). The results with HeLa cells on the one hand, and insulin-producing β-cells on the other hand, reflect their opposed metabolic phenotypes. While HeLa cells produce ATP mainly via glycolysis, β-cells produce large amounts of ATP via high rates of mitochondrial respiration.

The same protocol was used to investigate the effect of mitofusin 2 (Mfn2) ablation on energy metabolism. Mfn2 is involved in mitochondrial fusion and MAM formation (88–90), and its absence is also associated with considerable changes in cell bioenergetics (91). However, while Zorzano et al. (91) showed that Mfn2 silencing reduced oxygen

consumption, data from Mfn2 knockout cells from Kawalec et al. (92) indicate increased respiratory activity. Kawalec et al. explain this observation by an adaptation mechanism in the stable knockout cells. Also in my work, stable Mfn2 knockout cells were metabolically characterized with the help of mitochondrial ATP measurements. The results are in line with the observations of Kawalec et al. (92), showing higher ATP production via mitochondrial respiration compared to wild-type MEFs (42). Probably the short-term effects of the transient Mfn2 knockdown are different from the long-term effects, which are observed in stable Mfn2 knockout cells. However, further studies will be required to explain the consequences of Mfn2 ablation on cell metabolism.

In addition to the widely used HeLa cancer cell line, mitochondrial ATP measurements were also applied to analyze the specific bioenergetics of other cancer cell lines, namely breast adenocarcinoma cells (SkBr3, MCF7, MDA-MB231), lung adenocarcinoma cells (A549, H1299, Calu-3) and neuroblastoma cells (SH-SY5Y) (42). With respect to the preferred energy producing pathway of a cell, mitochondrial ATP measurements revealed clear differences between the different cancer cell types, which were not well detectable using respirometry (Seahorse®). Furthermore, a closer look on the mitochondrial ATP responses of the analyzed cancer cells revealed a high variability between different cancer types, for example with regard to the hexokinase-associated mitochondrial ATP elevations. Thus, mitochondrial ATP measurements likely reflect the unique nature of each cancer. In line with previously published data on mitochondrial function in different breast cancer cells (121), mitochondrial ATP measurements revealed clear differences between so called triple negative breast cancer (TNBC) (e.g. MDA-MB231), a highly malignant breast cancer subtype, compared to receptor-positive subtypes (e.g. MCF7). MDA-MB231 cells produce ATP predominantly via glycolysis while the ATP synthase is mostly running in reverse mode, whereas MCF7 cells, in comparison, generate less ATP via glycolysis, but display significant levels of mitochondrial ATP production by the ATP synthase. Altogether, the mitochondrial ATP measurements presented in this work demonstrate that single cell analysis of intracellular metabolites could be very useful for the metabolic profiling of cancer cells. Although there was a clear tendency to glycolytic ATP production with low respiratory activity in most cancer cells, the responses varied considerably between the different cell

types and also among different cells of the same cell line. The detailed metabolic characterization of cancer cells, in particular on the level of single cells, will increase our understanding of their specific metabolism, which will help to choose optimal therapeutic strategies and to improve diagnostic efficiency.

4.5. Concluding remarks

During my PhD thesis I delved into the fascinating and complex world of cellular bioenergetics. By monitoring ATP fluctuations in living cells it was possible to gain new insights into energy producing pathways. One important achievement of this work was to demonstrate that the real-time observation of intracellular molecules is a valuable tool for the investigation of cell physiological processes. For example, ATP measurements revealed new aspects regarding the role of mitochondria in cancer cell metabolism. In addition, details of the results presented in this thesis turned out to be particularly thought-provoking, thereby creating many interesting questions for follow-up studies.

5. Bibliography

1. Liberti MV, Locasale JW. The Warburg Effect: How Does it Benefit Cancer Cells? Trends Biochem Sci. 2016 Mar;41(3):211–8.

2. Warburg O. The Metabolism of Carcinoma Cells. J Cancer Res. 1925 Mar 1;9(1):148–63.

3. Warburg O, Posener K, Negelein, E. Über den Stoffwechsel der Tumoren. Biochem Z. 1924;152(1):319–44.

4. Warburg O, Wind F, Negelein E. THE METABOLISM OF TUMORS IN THE BODY. J Gen Physiol. 1927 Mar 7;8(6):519–30.

5. Dashty M. A quick look at biochemistry: Carbohydrate metabolism. Clin Biochem. 2013 Oct 1;46(15):1339–52.

6. Papa S, Capitanio G, Papa F. The mechanism of coupling between oxido-reduction and proton translocation in respiratory chain enzymes. Biol Rev. 2018 Feb 1;93(1):322–49.

7. Jonckheere AI, Smeitink JAM, Rodenburg RJT. Mitochondrial ATP synthase: architecture, function and pathology. J Inherit Metab Dis. 2012 Mar;35(2):211–25.

8. Walker JE. The ATP synthase: the understood, the uncertain and the unknown. Biochem Soc Trans. 2013 Feb 1;41(1):1–16.

9. Wilson JE. Isozymes of mammalian hexokinase: structure, subcellular localization and metabolic function. J Exp Biol. 2003 Jun;206(Pt 12):2049–57.

10. Robey RB, Hay N. Mitochondrial hexokinases, novel mediators of the antiapoptotic effects of growth factors and Akt. Oncogene. 2006 Aug 7;25(34):4683–96.

11. Goodpaster BH, Sparks LM. Metabolic Flexibility in Health and Disease. Cell Metab. 2017 May 2;25(5):1027–36.

12. Obre E, Rossignol R. Emerging concepts in bioenergetics and cancer research: Metabolic flexibility, coupling, symbiosis, switch, oxidative tumors, metabolic remodeling, signaling and bioenergetic therapy. Int J Biochem Cell Biol. 2015 Feb 1;59:167–81.

13. Van den Bossche J, O'Neill LA, Menon D. Macrophage Immunometabolism: Where Are We (Going)? Trends Immunol. 2017 Jun;38(6):395–406.

14. Seyfried TN, Flores RE, Poff AM, D'Agostino DP. Cancer as a metabolic disease: implications for novel therapeutics. Carcinogenesis. 2014 Mar;35(3):515–27.

15. Hanahan D, Weinberg RA. Hallmarks of Cancer: The Next Generation. Cell. 2011 Mar 4;144(5):646–74.

16. Pavlova NN, Thompson CB. The Emerging Hallmarks of Cancer Metabolism. Cell Metab. 2016 Jan 12;23(1):27–47.

17. Vander Heiden MG, DeBerardinis RJ. Understanding the Intersections between Metabolism and Cancer Biology. Cell. 2017 Feb 9;168(4):657–69.

18. Gentric G, Mieulet V, Mechta-Grigoriou F. Heterogeneity in Cancer Metabolism: New Concepts in an Old Field. Antioxid Redox Signal. 2016 May 26;26(9):462–85.

19. DeBerardinis RJ, Chandel NS. Fundamentals of cancer metabolism. Sci Adv. 2016 May 1;2(5):e1600200.

20. Warburg O. On the Origin of Cancer Cells. Science. 1956 Feb 24;123(3191):309–14.

21. Lunt SY, Vander Heiden MG. Aerobic Glycolysis: Meeting the Metabolic Requirements of Cell Proliferation. Annu Rev Cell Dev Biol. 2011 Oct 10;27(1):441–64.

22. Brand KA, Hermfisse U. Aerobic glycolysis by proliferating cells: a protective strategy against reactive oxygen species. FASEB J Off Publ Fed Am Soc Exp Biol. 1997;5:388–95.

23. Gatenby RA, Gillies RJ. Why do cancers have high aerobic glycolysis? Nat Rev Cancer. 2004 Nov;4(11):891–9.

24. Moreno-Sánchez R, Marín-Hernández A, Saavedra E, Pardo JP, Ralph SJ, Rodríguez-Enríquez S. Who controls the ATP supply in cancer cells? Biochemistry lessons to understand cancer energy metabolism. Int J Biochem Cell Biol. 2014 May 1;50:10–23.

25. Zu XL, Guppy M. Cancer metabolism: facts, fantasy, and fiction. Biochem Biophys Res Commun. 2004 Jan 16;313(3):459–65.

26. Pfeiffer T, Schuster S, Bonhoeffer S. Cooperation and Competition in the Evolution of ATP-Producing Pathways. Science. 2001 Apr 20;292(5516):504–7.

27. Altman BJ, Stine ZE, Dang CV. From Krebs to clinic: glutamine metabolism to cancer therapy. Nat Rev Cancer. 2016 Oct;16(10):619–34.

28. Hensley CT, Wasti AT, DeBerardinis RJ. Glutamine and cancer: cell biology, physiology, and clinical opportunities. J Clin Invest. 2013 Sep 3;123(9):3678–84.

29. DeBerardinis RJ, Cheng T. Q's next: the diverse functions of glutamine in metabolism, cell biology and cancer. Oncogene. 2010 Jan;29(3):313–24.

30. Vyas S, Zaganjor E, Haigis MC. Mitochondria and Cancer. Cell. 2016 Jul 28;166(3):555–66.

31. Valcarcel-Jimenez L, Gaude E, Torrano V, Frezza C, Carracedo A. Mitochondrial Metabolism: Yin and Yang for Tumor Progression. Trends Endocrinol Metab. 2017 Oct 1;28(10):748–57.

32. Zong W-X, Rabinowitz JD, White E. Mitochondria and Cancer. Mol Cell. 2016 Mar 3;61(5):667–76.

33. Spinelli JB, Haigis MC. The multifaceted contributions of mitochondria to cellular metabolism. Nat Cell Biol. 2018 Jul;20(7):745–54.

34. Schell JC, Olson KA, Jiang L, Hawkins AJ, Van Vranken JG, Xie J, et al. A Role for the Mitochondrial Pyruvate Carrier as a Repressor of the Warburg Effect and Colon Cancer Cell Growth. Mol Cell. 2014 Nov 6;56(3):400–13.

35. Christofk HR, Vander Heiden MG, Harris MH, Ramanathan A, Gerszten RE, Wei R, et al. The M2 splice isoform of pyruvate kinase is important for cancer metabolism and tumour growth. Nature. 2008 Mar;452(7184):230–3.

36. Stine ZE, Walton ZE, Altman BJ, Hsieh AL, Dang CV. MYC, Metabolism, and Cancer. Cancer Discov. 2015 Oct 1;5(10):1024–39.

37. Mullen AR, Hu Z, Shi X, Jiang L, Boroughs LK, Kovacs Z, et al. Oxidation of Alpha-Ketoglutarate Is Required for Reductive Carboxylation in Cancer Cells with Mitochondrial Defects. Cell Rep. 2014 Jun 12;7(5):1679–90.

38. Mullen AR, Wheaton WW, Jin ES, Chen P-H, Sullivan LB, Cheng T, et al. Reductive carboxylation supports growth in tumour cells with defective mitochondria. Nature. 2012 Jan;481(7381):385–8.

39. Gaude E, Frezza C. Defects in mitochondrial metabolism and cancer. Cancer Metab. 2014 Jul 17;2(1):10.

40. Chatterjee A, Mambo E, Sidransky D. Mitochondrial DNA mutations in human cancer. Oncogene. 2006 Aug;25(34):4663–74.

41. Sullivan LB, Chandel NS. Mitochondrial reactive oxygen species and cancer. Cancer Metab. 2014 Nov 28;2(1):17.

42. Depaoli MR, Karsten F, Madreiter-Sokolowski CT, Klec C, Gottschalk B, Bischof H, et al. Real-time imaging of mitochondrial ATP dynamics discloses the metabolic setting of single cells. Cell Rep. 2018 Oct 9;

43. Pak YL, Swamy KMK, Yoon J. Recent Progress in Fluorescent Imaging Probes. Sensors. 2015 Sep 22;15(9):24374–96.

44. Wu D, Sedgwick AC, Gunnlaugsson T, Akkaya EU, Yoon J, James TD. Fluorescent chemosensors: the past, present and future. Chem Soc Rev. 2017 Nov 27;46(23):7105–23.

45. Sanford L, Palmer A. Recent Advances in Development of Genetically Encoded Fluorescent Sensors. Methods Enzymol. 2017;589:1–49.

46. Perry SW, Norman JP, Barbieri J, Brown EB, Gelbard HA. Mitochondrial membrane potential probes and the proton gradient: a practical usage guide. BioTechniques. 2011 Feb 1;50(2):98–115.

47. Zhang X, Gao F. Imaging mitochondrial reactive oxygen species with fluorescent probes: Current applications and challenges. Free Radic Res. 2015 Apr 3;49(4):374–82.

48. Li H, Wan A. Fluorescent probes for real-time measurement of nitric oxide in living cells. Analyst. 2015 Oct 12;140(21):7129–41.

49. McQuade LE, Lippard SJ. Fluorescent probes to investigate nitric oxide and other reactive nitrogen species in biology (truncated form: fluorescent probes of reactive nitrogen species). Curr Opin Chem Biol. 2010 Feb 1;14(1):43–9.

50. Takanaga H, Chaudhuri B, Frommer WB. GLUT1 and GLUT9 as major contributors to glucose influx in HepG2 cells identified by a high sensitivity intramolecular FRET glucose sensor. Biochim Biophys Acta. 2008 Apr;1778(4):1091–9.

51. Imamura H, Nhat KPH, Togawa H, Saito K, Iino R, Kato-Yamada Y, et al. Visualization of ATP levels inside single living cells with fluorescence resonance energy transfer-based genetically encoded indicators. Proc Natl Acad Sci U S A. 2009 Sep 15;106(37):15651–6.

52. Vishnu N, Jadoon Khan M, Karsten F, Groschner LN, Waldeck-Weiermair M, Rost R, et al. ATP increases within the lumen of the endoplasmic reticulum upon intracellular Ca2+ release. Mol Biol Cell. 2014 Feb;25(3):368–79.

53. Yaginuma H, Kawai S, Tabata KV, Tomiyama K, Kakizuka A, Komatsuzaki T, et al. Diversity in ATP concentrations in a single bacterial cell population revealed by quantitative single-cell imaging. Sci Rep. 2014 Oct 6;4:6522.

54. Berg J, Hung YP, Yellen G. A genetically encoded fluorescent reporter of ATP:ADP ratio. Nat Methods. 2009 Feb;6(2):161–6.

55. Tantama M, Martínez-François JR, Mongeon R, Yellen G. Imaging energy status in live cells with a fluorescent biosensor of the intracellular ATP-to-ADP ratio. Nat Commun. 2013 Oct 7;4:2550.

56. Yoshida T, Alfaqaan S, Sasaoka N, Imamura H. Application of FRET-Based Biosensor “ATeam” for Visualization of ATP Levels in the Mitochondrial Matrix of Living Mammalian Cells. Methods Mol Biol Clifton NJ. 2017;1567:231–43.

57. Hung YP, Albeck JG, Tantama M, Yellen G. Imaging Cytosolic NADH-NAD+ Redox State with a Genetically Encoded Fluorescent Biosensor. Cell Metab. 2011 Oct 5;14(4):545–54.

58. Zhao Y, Hu Q, Cheng F, Su N, Wang A, Zou Y, et al. SoNar, a Highly Responsive NAD+/NADH Sensor, Allows High-Throughput Metabolic Screening of Anti-tumor Agents. Cell Metab. 2015 May 5;21(5):777–89.

59. Zhao Y, Wang A, Zou Y, Su N, Loscalzo J, Yang Y. *In vivo* monitoring of cellular energy metabolism using SoNar, a highly responsive sensor for NAD^+/NADH redox state. Nat Protoc. 2016 Aug;11(8):1345–59.

60. Eroglu E, Gottschalk B, Charoensin S, Blass S, Bischof H, Rost R, et al. Development of novel FP-based probes for live-cell imaging of nitric oxide dynamics. Nat Commun. 2016 Feb 4;7:10623.

61. Eroglu E, Rost R, Bischof H, Blass S, Schreilechner A, Gottschalk B, et al. Application of Genetically Encoded Fluorescent Nitric Oxide (NO•) Probes, the geNOps, for Real-time Imaging of NO• Signals in Single Cells. JoVE J Vis Exp. 2017 Mar 16;(121):e55486–e55486.

62. Eroglu E, Charoensin S, Bischof H, Ramadani J, Gottschalk B, Depaoli MR, et al. Genetic biosensors for imaging nitric oxide in single cells. Free Radic Biol Med [Internet]. 2018 Feb 2 [cited 2018 Sep 26]; Available from: http://www.sciencedirect.com/science/article/pii/S0891584918300376

63. Suzuki J, Kanemaru K, Iino M. Genetically Encoded Fluorescent Indicators for Organellar Calcium Imaging. Biophys J. 2016 Sep 20;111(6):1119–31.

64. Horikawa K. Recent progress in the development of genetically encoded Ca2+ indicators. J Med Invest. 2015;62(1.2):24–8.

65. Bischof H, Rehberg M, Stryeck S, Artinger K, Eroglu E, Waldeck-Weiermair M, et al. Novel genetically encoded fluorescent probes enable real-time detection of potassium in vitro and in vivo. Nat Commun. 2017 Nov 10;8(1):1422.

66. Poburko D, Santo-Domingo J, Demaurex N. Dynamic Regulation of the Mitochondrial Proton Gradient during Cytosolic Calcium Elevations. J Biol Chem. 2011 Jan 4;286(13):11672–84.

67. Tantama M, Hung YP, Yellen G. Imaging Intracellular pH in Live Cells with a Genetically Encoded Red Fluorescent Protein Sensor. J Am Chem Soc. 2011 Jul 6;133(26):10034–7.

68. Rupprecht C, Wingen M, Potzkei J, Gensch T, Jaeger K-E, Drepper T. A novel FbFP-based biosensor toolbox for sensitive in vivo determination of intracellular pH. J Biotechnol. 2017 Sep 20;258:25–32.

69. Sarkar AR, Heo CH, Xu L, Lee HW, Si HY, Byun JW, et al. A ratiometric two-photon probe for quantitative imaging of mitochondrial pH values. Chem Sci. 2015 Dec 17;7(1):766–73.

70. Pouvreau S. Genetically encoded reactive oxygen species (ROS) and redox indicators. Biotechnol J. 2014 Feb 1;9(2):282–93.

71. Tsou P, Zheng B, Hsu C-H, Sasaki AT, Cantley LC. A Fluorescent Reporter of AMPK Activity and Cellular Energy Stress. Cell Metab. 2011 Apr 6;13(4):476–86.

72. Takemoto K, Nagai T, Miyawaki A, Miura M. Spatio-temporal activation of caspase revealed by indicator that is insensitive to environmental effects. J Cell Biol. 2003 Jan 20;160(2):235–43.

73. Liu T, Yamaguchi Y, Shirasaki Y, Shikada K, Yamagishi M, Hoshino K, et al. Single-Cell Imaging of Caspase-1 Dynamics Reveals an All-or-None Inflammasome Signaling Response. Cell Rep. 2014 Aug 21;8(4):974–82.

74. Bajar BT, Lam AJ, Badiee RK, Oh Y-H, Chu J, Zhou XX, et al. Fluorescent indicators for simultaneous reporting of all four cell cycle phases. Nat Methods. 2016 Dec;13(12):993–6.

75. Sakaue-Sawano A, Kurokawa H, Morimura T, Hanyu A, Hama H, Osawa H, et al. Visualizing Spatiotemporal Dynamics of Multicellular Cell-Cycle Progression. Cell. 2008 Feb 8;132(3):487–98.

76. Nagai T, Sawano A, Park ES, Miyawaki A. Circularly permuted green fluorescent proteins engineered to sense Ca2+. Proc Natl Acad Sci. 2001 Mar 13;98(6):3197–202.

77. Nakai J, Ohkura M, Imoto K. A high signal-to-noise Ca^{2+} probe composed of a single green fluorescent protein. Nat Biotechnol. 2001 Feb;19(2):137–41.

78. Shrestha D, Jenei A, Nagy P, Vereb G, Szöllősi J. Understanding FRET as a Research Tool for Cellular Studies. Int J Mol Sci. 2015 Mar 25;16(4):6718–56.

79. Hochreiter B, Pardo-Garcia A, Schmid JA. Fluorescent Proteins as Genetically Encoded FRET Biosensors in Life Sciences. Sensors. 2015 Oct 16;15(10):26281–314.

80. Sun L, Shukair S, Naik TJ, Moazed F, Ardehali H. Glucose Phosphorylation and Mitochondrial Binding Are Required for the Protective Effects of Hexokinases I and II. Mol Cell Biol. 2008 Feb 1;28(3):1007–17.

81. Arora KK, Pedersen PL. Functional significance of mitochondrial bound hexokinase in tumor cell metabolism. Evidence for preferential phosphorylation of glucose by intramitochondrially generated ATP. J Biol Chem. 1988 Nov 25;263(33):17422–8.

82. Nelson BD, Kabir F. The role of the mitochondrial outer membrane in energy metabolism of tumor cells. Biochimie. 1986 Mar;68(3):407–15.

83. Roberts DJ, Miyamoto S. Hexokinase II integrates energy metabolism and cellular protection: Akting on mitochondria and TORCing to autophagy. Cell Death Differ. 2015 Feb;22(2):248–57.

84. Pedersen PL. Voltage dependent anion channels (VDACs): a brief introduction with a focus on the outer mitochondrial compartment's roles together with hexokinase-2 in the "Warburg effect" in cancer. J Bioenerg Biomembr. 2008 Jun;40(3):123–6.

85. Bronk SF, Gores GJ. Efflux of protons from acidic vesicles contributes to cytosolic acidification of hepatocytes during ATP depletion. Hepatology. 1991 Oct 1;14(4):626–33.

86. Devenish RJ, Prescott M, Boyle GM, Nagley P. The oligomycin axis of mitochondrial ATP synthase: OSCP and the proton channel. J Bioenerg Biomembr. 2000 Oct;32(5):507–15.

87. Miyoshi H, Tokutake N, Imaeda Y, Akagi T, Iwamura H. A model of antimycin A binding based on structure-activity studies of synthetic antimycin A analogues. Biochim Biophys Acta. 1995 Apr 26;1229(2):149–54.

88. Chen H, Detmer SA, Ewald AJ, Griffin EE, Fraser SE, Chan DC. Mitofusins Mfn1 and Mfn2 coordinately regulate mitochondrial fusion and are essential for embryonic development. J Cell Biol. 2003 Jan 20;160(2):189–200.

89. de Brito OM, Scorrano L. Mitofusin 2 tethers endoplasmic reticulum to mitochondria. Nature. 2008 Dec 4;456(7222):605–10.

90. Filadi R, Greotti E, Turacchio G, Luini A, Pozzan T, Pizzo P. Mitofusin 2 ablation increases endoplasmic reticulum-mitochondria coupling. Proc Natl Acad Sci U S A. 2015 Apr 28;112(17):E2174-2181.

91. Zorzano A, Hernández-Alvarez MI, Sebastián D, Muñoz JP. Mitofusin 2 as a driver that controls energy metabolism and insulin signaling. Antioxid Redox Signal. 2015 Apr 20;22(12):1020–31.

92. Kawalec M, Boratyńska-Jasińska A, Beręsewicz M, Dymkowska D, Zabłocki K, Zabłocka B. Mitofusin 2 Deficiency Affects Energy Metabolism and Mitochondrial Biogenesis in MEF Cells. PloS One. 2015;10(7):e0134162.

93. Vander Heiden MG, Cantley LC, Thompson CB. Understanding the Warburg effect: the metabolic requirements of cell proliferation. Science. 2009 May 22;324(5930):1029–33.

94. Herzig S, Shaw RJ. AMPK: guardian of metabolism and mitochondrial homeostasis. Nat Rev Mol Cell Biol. 2017 Oct 4;

95. Hardie DG, Lin S-C. AMP-activated protein kinase - not just an energy sensor. F1000Research. 2017;6:1724.

96. Chevrollier A, Loiseau D, Reynier P, Stepien G. Adenine nucleotide translocase 2 is a key mitochondrial protein in cancer metabolism. Biochim Biophys Acta. 2011 Jun;1807(6):562–7.

97. Gao H-Y, Luo X-G, Chen X, Wang J-H. Identification of key genes affecting disease free survival time of pediatric acute lymphoblastic leukemia based on bioinformatic analysis. Blood Cells Mol Dis. 2015 Jan 1;54(1):38–43.

98. Ureta T. The role of isozymes in metabolism: a model of metabolic pathways as the basis for the biological role of isozymes. Curr Top Cell Regul. 1978;13:233–58.

99. Ovádi J, Srere PA. Macromolecular compartmentation and channeling. Int Rev Cytol. 2000;192:255–80.

100. Meurer F, Bobrownik M, Sadowski G, Held C. Standard Gibbs Energy of Metabolic Reactions: I. Hexokinase Reaction. Biochemistry (Mosc). 2016 Oct 11;55(40):5665–74.

101. Chinopoulos C. Mitochondrial consumption of cytosolic ATP: not so fast. FEBS Lett. 2011 May 6;585(9):1255–9.

102. Pastorino JG, Shulga N, Hoek JB. Mitochondrial Binding of Hexokinase II Inhibits Bax-induced Cytochrome c Release and Apoptosis. J Biol Chem. 2002 Jan 3;277(9):7610–8.

103. Chiara F, Castellaro D, Marin O, Petronilli V, Brusilow WS, Juhaszova M, et al. Hexokinase II Detachment from Mitochondria Triggers Apoptosis through the Permeability Transition Pore Independent of Voltage-Dependent Anion Channels. PLOS ONE. 2008 Mar 19;3(3):e1852.

104. Majewski N, Nogueira V, Bhaskar P, Coy PE, Skeen JE, Gottlob K, et al. Hexokinase-Mitochondria Interaction Mediated by Akt Is Required to Inhibit Apoptosis in the Presence or Absence of Bax and Bak. Mol Cell. 2004 Dec 3;16(5):819–30.

105. Gall JM, Wong V, Pimental DR, Havasi A, Wang Z, Pastorino JG, et al. Hexokinase regulates Bax-mediated mitochondrial membrane injury following ischemic stress. Kidney Int. 2011 Jun 1;79(11):1207–16.

106. Pastorino JG, Hoek JB. Hexokinase II: the integration of energy metabolism and control of apoptosis. Curr Med Chem. 2003 Aug;10(16):1535–51.

107. Majewski N, Nogueira V, Robey RB, Hay N. Akt Inhibits Apoptosis Downstream of BID Cleavage via a Glucose-Dependent Mechanism Involving Mitochondrial Hexokinases. Mol Cell Biol. 2004 Jan 15;24(2):730–40.

108. Wu R, Wyatt E, Chawla K, Tran M, Ghanefar M, Laakso M, et al. Hexokinase II knockdown results in exaggerated cardiac hypertrophy via increased ROS production. EMBO Mol Med. 2012 Jul 3;4(7):633–46.

109. Baines CP. The Cardiac Mitochondrion: Nexus of Stress. Annu Rev Physiol. 2010;72(1):61–80.

110. da-Silva WS, Gómez-Puyou A, de Gómez-Puyou MT, Moreno-Sanchez R, De Felice FG, de Meis L, et al. Mitochondrial bound hexokinase activity as a preventive antioxidant defense: steady-state ADP formation as a regulatory mechanism of membrane potential and reactive oxygen species generation in mitochondria. J Biol Chem. 2004 Sep 17;279(38):39846–55.

111. McCommis KS, Douglas DL, Krenz M, Baines CP. Cardiac-specific hexokinase 2 overexpression attenuates hypertrophy by increasing pentose phosphate pathway flux. J Am Heart Assoc. 2013 Nov 4;2(6):e000355.

112. Río Bártulos C, Rogers MB, Williams TA, Gentekaki E, Brinkmann H, Cerff R, et al. Mitochondrial Glycolysis in a Major Lineage of Eukaryotes. Genome Biol Evol. 2018 Sep 1;10(9):2310–25.

113. Opperdoes FR, Borst P. Localization of nine glycolytic enzymes in a microbody-like organelle in Trypanosoma brucei: The glycosome. FEBS Lett. 1977 Aug 15;80(2):360–4.

114. Michels PAM, Bringaud F, Herman M, Hannaert V. Metabolic functions of glycosomes in trypanosomatids. Biochim Biophys Acta BBA - Mol Cell Res. 2006 Dec 1;1763(12):1463–77.

115. Jang S, Nelson JC, Bend EG, Rodríguez-Laureano L, Tueros FG, Cartagenova L, et al. Glycolytic Enzymes Localize to Synapses under Energy Stress to Support Synaptic Function. Neuron. 2016 Apr 20;90(2):278–91.

116. Burté F, Carelli V, Chinnery PF, Yu-Wai-Man P. Disturbed mitochondrial dynamics and neurodegenerative disorders. Nat Rev Neurol. 2015 Jan;11(1):11–24.

117. Lin M-Y, Sheng Z-H. Regulation of mitochondrial transport in neurons. Exp Cell Res. 2015 May 15;334(1):35–44.

118. Schwarz TL. Mitochondrial Trafficking in Neurons. Cold Spring Harb Perspect Biol. 2013 Jan 6;5(6):a011304.

119. Giegé P, Heazlewood JL, Roessner-Tunali U, Millar AH, Fernie AR, Leaver CJ, et al. Enzymes of Glycolysis Are Functionally Associated with the Mitochondrion in Arabidopsis Cells. Plant Cell. 2003 Sep 1;15(9):2140–51.

120. Graham JWA, Williams TCR, Morgan M, Fernie AR, Ratcliffe RG, Sweetlove LJ. Glycolytic Enzymes Associate Dynamically with Mitochondria in Response to Respiratory Demand and Support Substrate Channeling. Plant Cell. 2007 Nov 1;19(11):3723–38.

121. Pelicano H, Zhang W, Liu J, Hammoudi N, Dai J, Xu R-H, et al. Mitochondrial dysfunction in some triple-negative breast cancer cell lines: role of mTOR pathway and therapeutic potential. Breast Cancer Res BCR. 2014 Sep 11;16(5):434.